

## The Canadian Airport Nowcasting System (CAN-Now)

George A. Isaac,<sup>a,\*</sup> Monika Bailey,<sup>a</sup> Faisal S. Boudala,<sup>a</sup> William R. Burrows,<sup>a</sup> Stewart G. Cober,<sup>a</sup>  
Robert W. Crawford,<sup>a</sup> Norman Donaldson,<sup>a</sup> Ismail Gultepe,<sup>a</sup> Bjarne Hansen,<sup>a</sup> Ivan Heckman,<sup>a</sup> Laura X. Huang,<sup>a</sup>  
Alistair Ling,<sup>a</sup> Jocelyn Mailhot,<sup>b</sup> Jason A. Milbrandt,<sup>b</sup> Janti Reid<sup>a</sup> and Marc Fournier<sup>c</sup>

<sup>a</sup> Cloud Physics and Severe Weather Research Section, Environment Canada, Toronto, Canada

<sup>b</sup> Atmospheric Numerical Weather Prediction Research Section, Environment Canada, Montreal, Canada

<sup>c</sup> Canadian Meteorological Aviation Centre-East, Environment Canada, Montreal, Canada

**ABSTRACT:** The Canadian Airport Nowcasting Project (CAN-Now) has developed an advanced prototype all-season weather forecasting and nowcasting system that can be used at major airports. This system uses numerical model data, pilot reports, ground *in situ* sensor observations (precipitation, icing, ceiling, visibility, winds), on-site remote sensing (such as vertically pointing radar and microwave radiometer) and off-site remote sensing (satellite and radar) information to provide detailed nowcasts out to approximately 6 h. The nowcasts, or short term weather forecasts, should allow decision makers such as pilots, dispatchers, de-icing crews, ground personnel or air traffic controllers to make plans with increased margins of safety and improved efficiency. The system has been developed and tested at Toronto Pearson International Airport (CYYZ) and Vancouver International Airport (CYVR). A Situation Chart has been developed to allow users to have a high glance value product which identifies significant weather related problems at the airport. New products combining observations and numerical model output into nowcasts have been tested. Some statistical verifications of forecast products, with comparisons to persistence, covering both a winter (2009/2010) and summer (2010) period have been made. Problems with the prediction of relative humidity and wind direction are outlined. The ability to forecast categorical variables such as ceiling, visibility, as well as precipitation rate and type accurately are discussed. Overall, for most variables, the nowcast systems can outperform persistence after the first 1 or 2 h, and provide more accurate forecasts than individual Numerical Weather Prediction models out to 6 h.

**KEY WORDS** nowcasting; weather forecasting; aviation; airport weather

Received 16 August 2011; Revised 14 May 2012; Accepted 21 May 2012

### 1. Introduction

Operations at airports are very sensitive to weather. This not only includes the obvious take-off and landing phases of aircraft operation, but also activities that are essential components of an airport such as active runway selection, snow removal, de-icing, and safety of ground personnel during lightning events. Many decisions are made that require weather information on short time scales. Nowcasting is weather forecasting on such short time scales, typically less than 6 h. The Canadian Airport Nowcasting (CAN-Now) project was initiated in 2006 to help address the need for improved short term weather forecasting. It is a follow-on to an earlier project, the Airport Vicinity Icing and Snow Advisor (AVISA; Isaac *et al.*, 2006). AVISA focused on icing at the airport but it was recognized that such a system would not be implemented unless it considered all potential weather hazards during every season. However, a report on CAN-Now which just focuses on the icing aloft and at the airport has been prepared (Isaac *et al.*, 2011).

The main objective of CAN-Now is to develop a four-season forecasting/nowcasting system at a major airport which will be

able to produce detailed nowcasts and forecasts of weather phenomena (see Table 1). This information should allow airport-related decision makers (pilots, dispatchers, de-icing crews, ground operations, air traffic control) to make decisions that have increased margins of safety and improved efficiency. For this project, Toronto Pearson International Airport (CYYZ) and Vancouver International Airport (CYVR) have been chosen to demonstrate such a system. The prototype nowcasts rely on existing routinely available weather information including Numerical Weather Prediction (NWP) model output, site climatologies, radar and lightning network observations, and measurements from on-site routine sensors (e.g. wind, precipitation, visibility, ceiling, temperature), augmented by specialized information from high resolution local area models and from high time resolution instrumentation such as microwave radiometers, vertically pointing radars and particle type sensors. The prototype system has run in a nowcasting mode for several years now, detecting weather hazards and providing forecasts out to about 3–6 h for most phenomena, and out to 36 h for some subsets of phenomena.

It should be mentioned that the climate of Canada does impose priorities for aviation forecasting that are different from other locations. For example, snow fall prediction is very important, even for airports such as Vancouver where it rarely occurs. These events slow down activity at the airport while runways are cleared, and aircraft de-iced. In many cases, extra personnel must be called in to perform these tasks. The air

\* Correspondence to: G. A. Isaac, Cloud Physics and Severe Weather Research Section, Environment Canada, Toronto M3H5T4, Canada. E-mail: george.isaac@ec.gc.ca

Table 1. Phenomena considered by the CAN-now system.

Snow and rain events
Freezing precipitation and ice pellets
Frost
Blowing snow
Icing aloft
High winds/gusts
Wind shifts/shear
Turbulence
Lightning
Low ceilings
Low visibility and fog
Convective cells

navigation authority in Canada, NAV CANADA (John Footitt, pers. comm.), indicates that crosswinds, or sudden wind shifts, that can close down certain runways and require a runway change remains their most important logistical concern affecting airport operations. In the summer, lightning in the vicinity of the airport can shut down the airport entirely because of safety concerns for ground personnel. For other climates, factors such as wind shear can be very important. However, dangerous wind shear events (for example microbursts) occur so infrequently at Canadian airports that no special warning systems such as a Terminal Doppler Weather Radar (TDWR; Turnbull *et al.*, 1989) or a low level wind shear alert system (LLWAS) have been purchased. The CAN-Now system was designed and tested after many discussions with potential users such as NAV CANADA, aviation weather forecasters, airline dispatchers, and airport authorities, and is tuned for mainly Canadian clients.

This paper introduces the current capabilities of CAN-Now and focuses on the winter 2009/2010 and summer 2010 verification of CAN-Now forecast products. It also describes future work that could be performed.

## 2. Basic design of CAN-Now system

It is known that persistence and trends of observations produce better forecasts than NWP models on very short time scales, and

numerical models produce more accurate forecasts on longer time scales, usually greater than 4–6 h (see Golding, 1998). CAN-Now blends observation and numerical model data to produce better nowcasts. A schematic view of CAN-Now is given in Figure 1.

Basically, the system ingests any information that is currently available. It uses the Canadian GEM Regional (REG) and Local Area (LAM) models which have been described by Côté *et al.* (1998a, 1998b) and Mailhot *et al.* (2006), and the U.S. Rapid Update Cycle 13 km (RUC) model described by Benjamin *et al.* (2004, 2006). These model data have the following spatial and temporal resolutions available to the system: REG (15 km, 7.5 min), LAM East (2.5 km, 5 min), LAM Olympic (2.5 km, 1 min), and RUC (13 km, hourly). This work also includes verification statistics of the LAM 1 km (LAM1K) model, however, it is not ingested into the system. Also note that only the 6 h RUC forecast is used in CAN-Now. The system integrates the data and applies a number of scientific algorithms to produce an increased set of weather parameters. Such aviation-relevant parameters include: visibility (Gultepe *et al.*, 2006; Boudala and Isaac, 2009; Gultepe and Milbrandt, 2010), wind gust (modified Brasseur, 2001), runway visual range (Boudala *et al.*, 2012), and precipitation type (Bourgouin, 2000 and direct model output). For ceiling, model estimates are based on simple thresholds. In REG cloud base occurs at the lowest level where the cloud fraction is greater than 0.01. In LAM, similar to RUC, cloud base is chosen at the lowest level where the cloud water mixing ratio is  $10^{-6}$  kg kg<sup>-1</sup>. Nowcasting methods then make use of the system inputs (model data and observations), plus the algorithm results, to generate new forecast products. The CAN-Now system also includes forecasts of ceiling and visibility obtained from an application that combines current conditions, conditional climatology and model-based conditions (Hansen, 2007). A web-based system is used for delivery of the products.

## 3. Observations at the airport

In addition to using the reports from the official human observers at both CYYZ and CYVR, instruments were

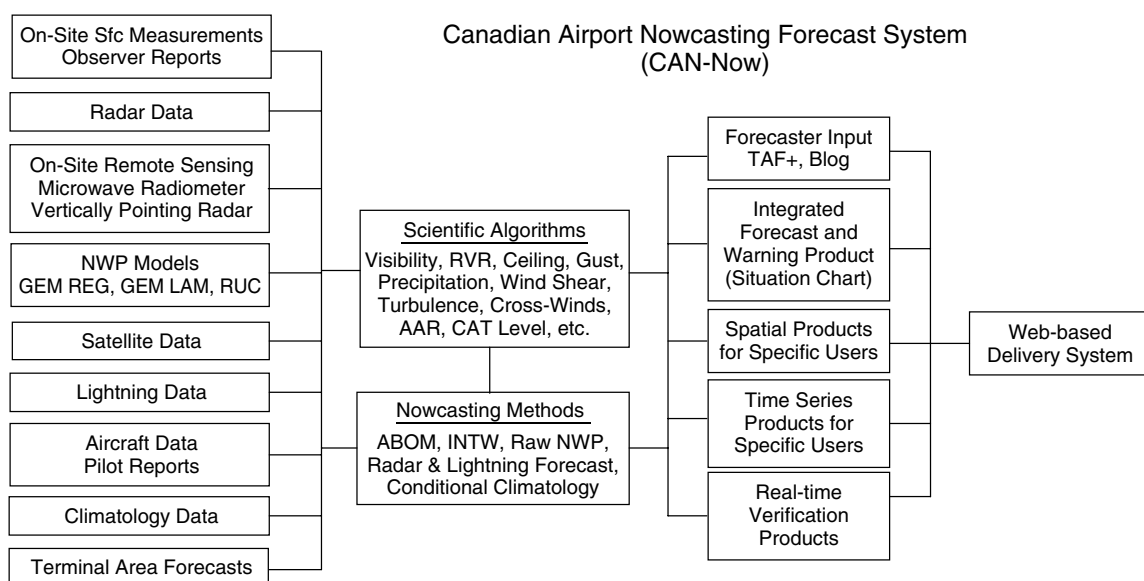


Figure 1. A schematic representation of CAN-Now. The abbreviations are described in the text.

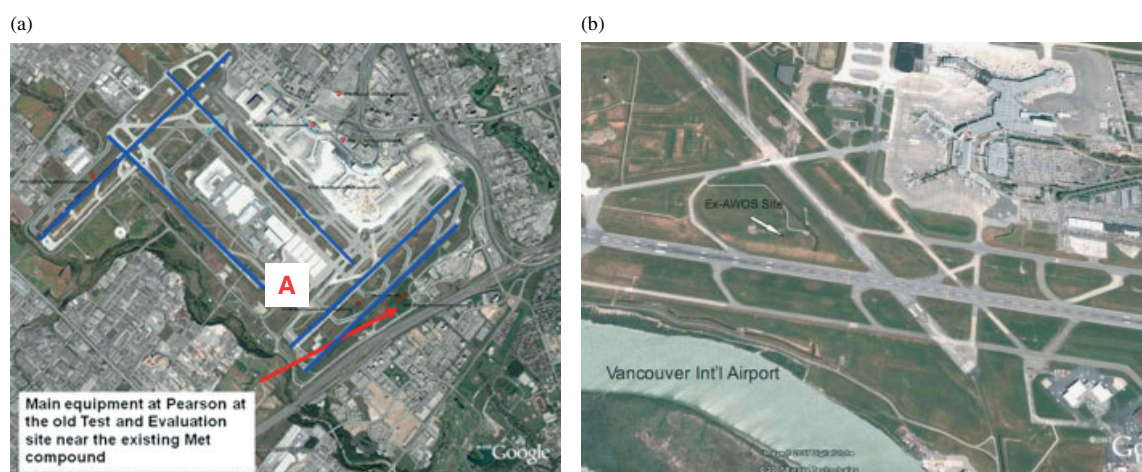


Figure 2. Shows the location of the on-site instruments installed at CYYZ (a) and CYVR (b) as marked on a Google Map. The major runways at CYYZ are highlighted in blue. The de-icing pad at CYYZ is marked with a letter A.

installed to obtain high temporal resolution measurements of temperature, relative humidity, wind speed and direction, ceiling, visibility, precipitation rate and type, as well as cameras that can monitor current conditions. Whenever possible, some of the parameters were measured by more than one instrument which increased the robustness of the system. At CYYZ, the largest HUB airport in Canada, some specialized instruments were installed, including a Vertically Pointing X-Band Radar, manufactured by McGill University, and a TP3000 profiling microwave radiometer from Radiometrics (Ware *et al.*, 2003). The instruments at CYYZ were located near the existing meteorological compound just off one of the main runways. At CYVR, the instruments were located between the major runways at an ex-AWOS instrument site (see Figure 2 and Table 2).

The data at both sites were recorded on-site and at the main project computer server. Most of the measurements were acquired at 1 min intervals. Experience has shown that there are many rapid fluctuations in variables such as wind speed and direction, visibility and ceiling which require 1 min data in order to obtain an accurate picture of what is happening at the airport.

Figure 3 shows sample products from the Vertically Pointing X-Band Radar installed at CYYZ. The products are based on work performed at McGill University by Zawadzki *et al.* (2001) and Lilly *et al.* (2004).

Figure 4 shows an example of a sounding produced by the Microwave Profiling Radiometer installed at CYYZ. It can produce time series of temperature, water vapour, and cloud liquid water content as a function of height and time. These products can be used to detect aircraft icing aloft and the stability of the atmosphere.

#### 4. Nowcast systems

Several short term weather forecasting or nowcasting systems have been developed for use with CAN-Now.

A radar extrapolation scheme moves radar echoes or precipitation echoes forward based on the history of their past motions. This gives approximately a 2 h 'nowcast' of precipitation that will occur at the airport. The system predicts the most likely precipitation rate, following a direct translation in time, as well as a possible maximum value obtained by scanning upstream

Table 2. List of specific instruments installed at CYVR and CYYZ for CAN-now.

Instrument	Vancouver (CYVR)	Pearson (CYYZ)
Flexwatch Camera System	1	1
Vaisala HPM45C212 Temperature and Relative Humidity	1	1
RM Young 61205V Barometric Pressure System	1	–
Met One Pressure Sensor	–	1
Vaisala CT25K Ceilometer	1	1
Vaisala FD12P Visibility and Present Weather Sensor	1	1
OTT Parsivel Present Weather Sensor	1	1
Yankee TPS3100 Hot Plate Precipitation Gauge	1	1
Belfort Precipitation Gauge with Nipher Shield	–	1
Hydrological Services TP3 Tipping Bucket Rain Gauge	1	1
Geonor T-200B Precipitation Gauge with Nipher Shield	1	1
Sonic Ranger SR50AT Snow Depth Sensor	1	1
Rosemount Icing Detector	–	1
Vaisala WS425 Ultra Sonic Wind Sensor	–	1
AES 78D Cup Anemometer	1	1
RM Young Model 05103-10 Wind Monitor	1	1
McGill X-Band Vertically Pointing Radar	–	1
Radiometric Passive Microwave Radiometer TP3000	–	1

directions for 8° on either side of the calculated direction of motion (using the calculated speed). This point forecast process is currently implemented in Environment Canada's Canadian Radar Decision Support (CARDS) system software and is based on the scheme developed by Bellon and Austin (1986). A similar scheme has been implemented in the Weather Support to Deicing Decision Making (WSDDM; Rasmussen *et al.*, 2001) system.

A lightning extrapolation scheme moves lightning stroke point locations forward in time for 2 h based on the NWP

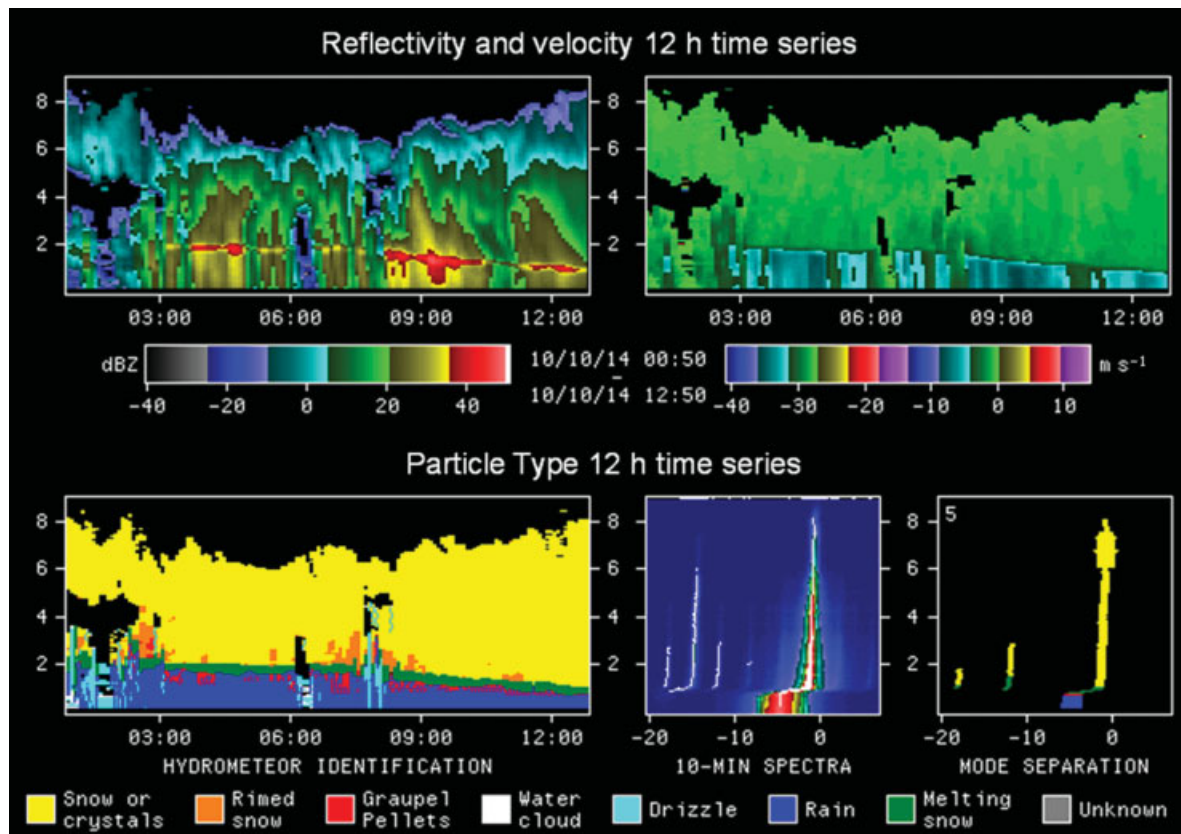


Figure 3. Example products from the Vertically Pointing X-Band Radar installed at CYYZ showing the vertical profile of radar reflectivity and Doppler velocity, as well as an interpretation of precipitation types and fall velocity spectra.

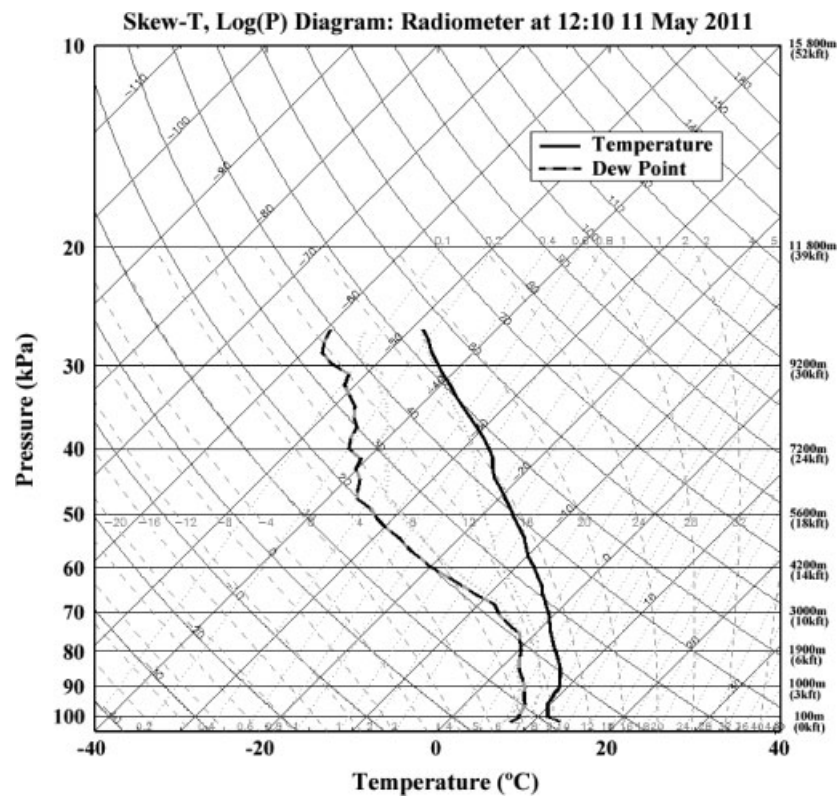


Figure 4. An example of a sounding from the Microwave Profiling Radiometer that can be produced every few minutes.



model wind field. Lightning information is obtained from the Canadian Lightning Detection Network which is part of the North American Lightning Detection Network operated by Vaisala (see Burrows and Kochtubajda, 2010).

The Weighting, Evaluation, Bias Correction and Integrated System for Nowcasting (WEBIS), or Integrated Weighting System (INTW; Huang, 2011; Huang *et al.*, 2012) for its short title, examines several different models, dynamically weighs those models based on recent performance (6 h), and applies dynamic and variational bias corrections to produce a short term forecast out to 6 h. The INTW system uses the REG, RUC, and LAM models, the 1 min data from the observation sites at CYYZ and CYVR, and the hourly observations from other sites.

A system called the Adaptive Blending of Observations and Models (ABOM; Bailey *et al.*, 2009) considers three parameters: the actual weather, a forecast change in weather extrapolating the past history of the observations, and a forecast change based on a numerical weather prediction model. It then applies weights to those parameters to produce a nowcast. The Numerical Weather Prediction models used are the same as

those for INTW but it looks at each model separately, either the Regional (ABOM REG) or Local Area Model (ABOM LAM). Verification of the lightning, ABOM and INTW systems will be presented in Section 7.

Some 'nowcasts' rely strictly on model predictions. For example, for turbulence, model produced Energy Dissipation Rates (EDR) and Momentum Fluxes (M. Flux) are used. Some crude wind shear forecasts are being made using the limits of greater than 25, 40 and 50 kt in the first 500, 100 and 1500 ft respectively as outlined in MANAIR (the manual of standards and procedures for aviation weather forecasts). These forecasts are based on model forecasts and whenever these thresholds are exceeded, some text is added to the appropriate line in the Situation Chart (Figure 5). However, wind shear is poorly predicted by the models (Zhou, 2010) and a warning is very rarely made. There are no special wind shear sensors at the airport. The nearby operational Doppler radar does produce charts warning of existing gust fronts, and mesocyclones and these are part of CAN-Now spatial products. However, no actual nowcasts are produced using the radar. The temporal resolution is not as good as

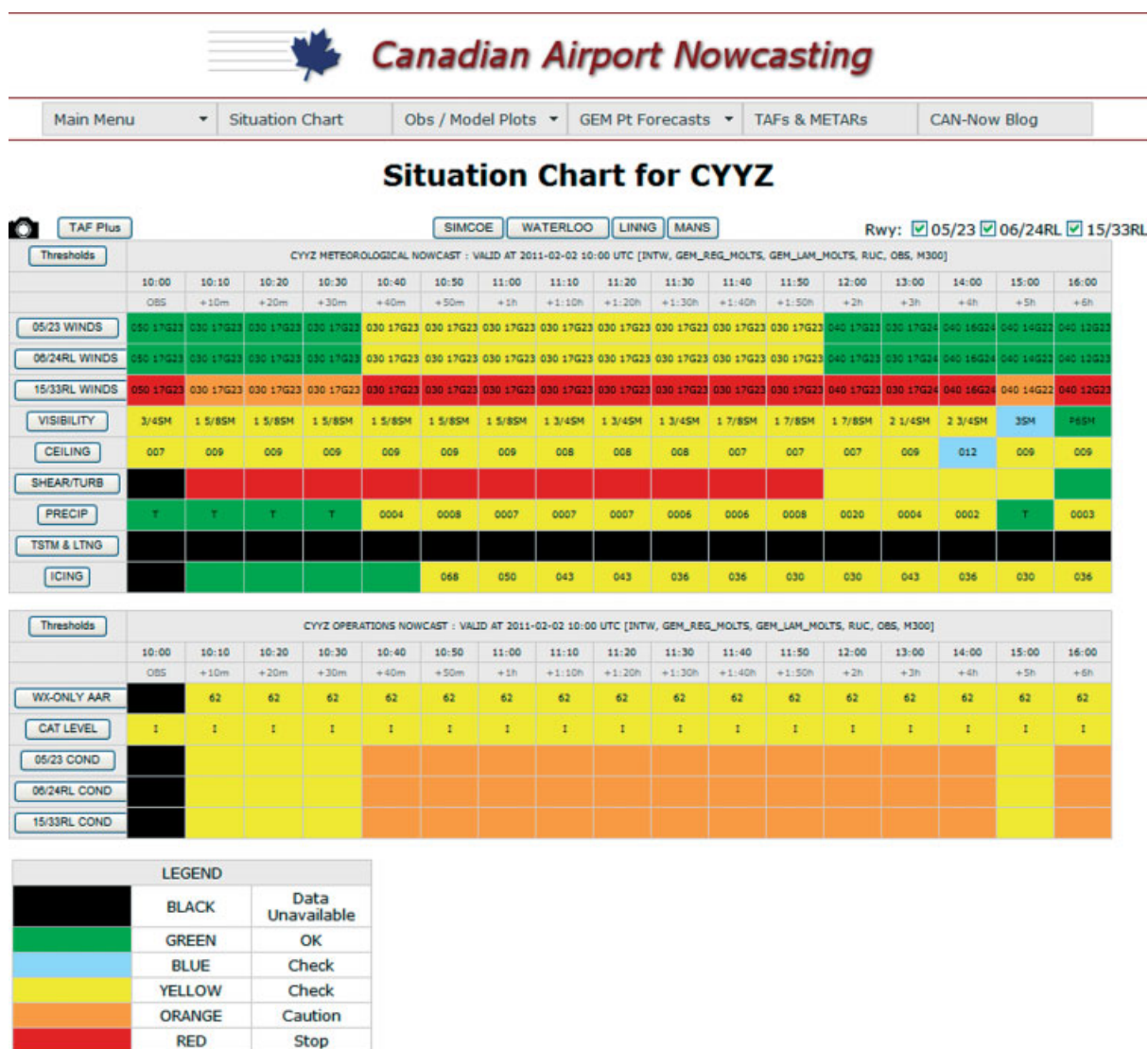


Figure 5. An example of the Situation Chart for CYYZ on 2 February 2011. Time bars are drawn at 10 min intervals for the first 2 h and then hourly out to 6 h. Parameters include crosswinds for three runway directions, visibility, ceiling, shear/turbulence, precipitation, thunderstorms and lightning and icing. A weather only Airport Arrival Rate (AAR), CAT level, and runway condition are also calculated.

typical wind shear systems such as TDWR and LLWAS. As mentioned above, the Canadian Air Navigation Authority, NAV CANADA, has not installed such systems at Canadian airports because the perceived wind shear threat is not considered large.

## 5. Sample products

The system produces the following products.

1. A web-based overview map of either CYYZ or CYVR with all their significant alternates (total 46 airports). Clicking on any of the airport symbols brings the user to a Situation Chart.

2. The Situation Chart (Figure 5), which is updated every 10 min, shows present weather and forecasts for crosswind for each airport runway, visibility, ceiling, shear/turbulence, precipitation, thunderstorms and lightning, icing aloft, weather-only arrival rate, CAT level, and runway condition. CAT Levels are used at airports with Instrument Landing Systems. The Categories or CAT I, II or III have different decision or ceiling heights and runway visual range thresholds (see Table 3(b)). The nowcasts include predictions for each 10 min in the first 2 h and then hourly out to 6 h. The forecasts on the Situation Chart change colour when certain thresholds are crossed as defined in a clickable table of thresholds (see Table 3(a) and (b) for examples). For CYYZ and CYVR, on-site cameras provide visual images of the weather, and a current enhanced forecast is available

Table 3a. Thresholds used in the situation chart.

Parameter	Units	Lower limit	Upper limit	Colour	Explanation
'Dry runway' crosswind	kt	25	–	Red	Not permitted
	kt	20	25	Orange	–
	kt	15	20	Yellow	–
	kt	0	15	Green	–
'Wet runway' crosswind	kt	15	–	Red	Not permitted
	kt	10	15	Orange	–
	kt	5	10	Yellow	–
	kt	0	5	Green	–
Visibility	SM	0	One fourth	Red	BLO landing
	SM	One fourth	One half	Orange	BLO alternate
	SM	One half	3	Yellow	IFR
	SM	3	6	Blue	MVFR
	SM	6	–	Green	VFR
Ceiling	ft	< 150	–	Red	BLO landing
	ft	150	400	Orange	BLO alternate
	ft	400	1000	Yellow	IFR
	ft	1000	2500	Blue	MVFR
	ft	2500	10 000	Green	VFR
	ft	–	≥ 10 000	Green	Unlimited
Shear/turbulence	$m^{2/3}s^{-1}$	–	Max EDR ≥ 0.5	Red	Severe
	Pa	–	M. Flux ≥ 1.5	Red	Severe
	$m^{2/3}s^{-1}$	Max EDR ≥ 0.3	Max EDR < 0.5	Yellow	Moderate
	Pa	M. Flux ≥ 0.75	M. Flux < 1.5	Yellow	Moderate
	$m^{2/3}s^{-1}$	Max EDR < 0.3	–	Green	Light
	Pa	M. Flux < 0.75	–	Green	Light
Precipitation	mm h <sup>-1</sup>	–	> 7.5	Red	Heavy
	mm h <sup>-1</sup>	2.5	7.5	Orange	Moderate
	mm h <sup>-1</sup>	0.2	2.5	Yellow	Light
	mm h <sup>-1</sup>	0	0.2	Green	Trace
	mm h <sup>-1</sup>	None	–	Green	None
Lightning	SM	–	< 6	Red	–
	SM	6	10	Orange	–
	SM	10	30	Yellow	–
	SM	< 273	–	Green	–
	SM	None	–	Green	–
Runway condition	mm h <sup>-1</sup>	0	0.2	Yellow	Possible dry
	mm h <sup>-1</sup>	> 0.2	–	Orange	Possible wet
Wx Only AAR	–	–	–	Red	Not permitted
	CAT IIIa	–	–	Red	–
	CAT II	–	–	Orange	–
	CAT I	–	–	Yellow	–
	VFR	–	–	Green	–

Note that 'Dry runway' is defined as precipitation rate ≤ 0.2 mm h<sup>-1</sup> and visibility ≥ 1 SM, and 'Wet runway' is defined as precipitation rate > 0.2 mm h<sup>-1</sup> or visibility < 1 SM. For icing, the time cell is labelled green if the total water content < 0.1 g m<sup>-3</sup> at temperatures < 0°C. If the total water content is higher than this at supercooled temperatures, the cell is coloured yellow.

Table 3b. Examples of thresholds used for CAT-level in the situation chart.

Parameter	RVR			Ceiling		Colour	Explanation
	Lower limit	Upper limit		Lower limit	Upper limit		
CAT-level	–	600 ft		–	–	Red	Not permitted
	600 ft	1200 ft	or	–	100 ft	Red	CAT IIIa
	1200 ft	2600 ft	or	100 ft	200 ft	Orange	CAT II
	2600 ft	3 SM	or	200 ft	1000 ft	Yellow	CAT I
	3 SM	6 SM	or	1000 ft	2500 ft	Blue	MVFR
	6 SM	–	and	2500 ft	–	Green	VFR

Note that predictions of RVR are necessary for the prediction of the CAT-level.

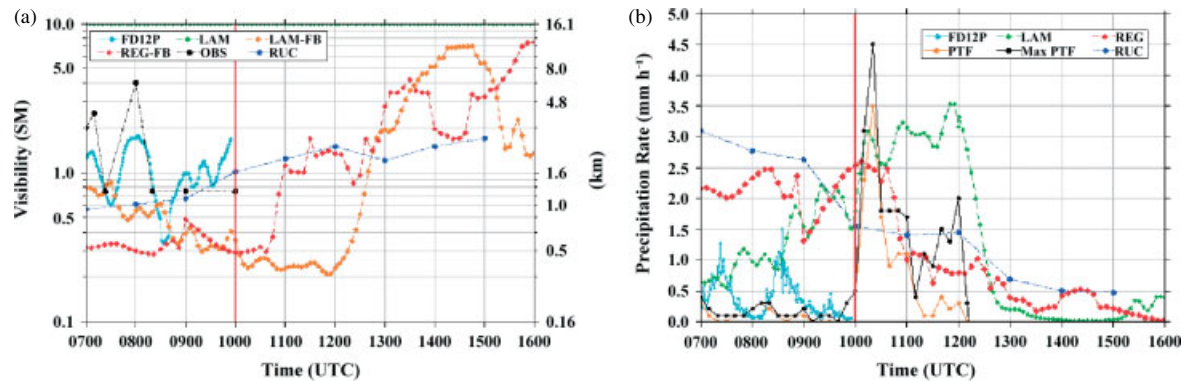


Figure 6. (a) Shows visibility as measured for the past 3 h (FD12P) and forecast for the next 6 h for 2 February 2011. The official observer observations are marked as black dots (OBS). The red vertical line indicates the current time. Predictions from the Canadian GEM Regional (REG) and Local Area Model (LAM) as well as the U.S. RUC model are included. (b) Shows precipitation rate in the same format as (a). Measurements from the Vaisala FD12P, the King City Radar precipitation point forecast (PTF) and maximum in an extrapolated arc (MAXPTF). The REG, the LAM, and RUC forecasts are plotted.

- from the Canadian Meteorological Aviation Centre. Forecasts for the ‘bedposts’ in the form of time-height plots can also be examined. Bedposts are terminal area entry locations and both CYYZ and CYVR have four such predefined locations.
- Charts showing observations and forecasts from the past 3 h, along with forecasts for the next 6 h are available (e.g. Figure 6(a) and (b)).
- Nowcasts using the ABOM and INTW techniques are also available (Figure 7(a) and (b)).
- Many spatial products such as scanning radar imagery, satellite imagery, pilot reports (PIREPs) and lightning charts.

- A suite of model forecasts out to 36 h.

## 6. Winter and summer verification of models

A verification of NWP models used in the CAN-Now system was done for the winter of 2009/2010 (1 December 2009 to 31 March 2010) and the summer of 2010 (1 June 2010 to 31 August 2010). This section presents only a small portion of those results. The models used, the model run times and resolution and the location of the model point used in the verification are given in Table 4.

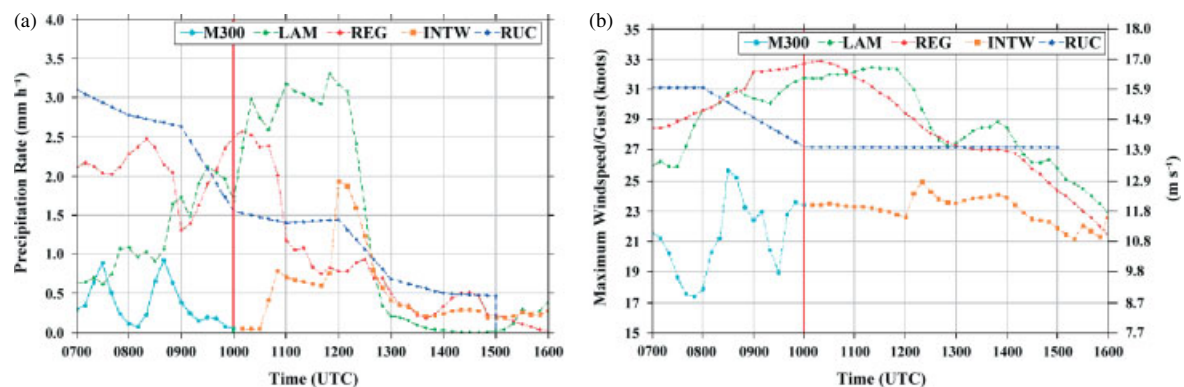


Figure 7. (a) Shows the precipitation nowcast plot showing the measurements (M300), the NWP model predictions and the INTW nowcast for 2 February 2011. (b) Shows the wind gust nowcast plot showing the NWP model forecasts along with the INTW nowcast. M300 refers to the data acquisition system for the on-site measurements. The vertical red line indicates the current time.

Table 4. A description of the NWP models used in the statistical analysis, including their spatial and temporal resolution and the actual location of the model grid point.

	Model run times (UTC)	Model resolution		Location	
		Horizontal	Temporal	CYYZ	CYVR
Actual geographic location	–	–	–	43.68, –79.63	49.19, –123.19
REG	0000, 0600, 1200, 1800	15 km	7.5 min	43.65, –79.68	49.22, –123.16
LAM (east)	1200	2.5 km	5 min	43.67, –79.63	–
LAM Olympic (west)	0900, 2100 up to 9 December 0600, 1500 afterwards	2.5 km	1 min	–	49.18, –123.19
LAM 1 km Olympic (west)	1100, 2300 up to 9 December 1100, 2000 afterwards	1 km	30 s	–	49.18, –123.17
RUC	Every hour	13 km	1 h	43.66, –79.70	49.19, –123.21

Note that although RUC model data are available hourly, only the RUC 6 h forecast was used in this work.

Model and instrument data were reduced to 10 min time intervals by using the last instantaneous value for all REG variables, and linearly interpolating RUC data to 10 min (although hourly RUC predictions are compared in this work). For LAM and instrument data, the average during the last 10 min for temperature, RH, wind speed, max wind, crosswinds, the minimum value during last 10 min for visibility and ceiling, the maximum value during last 10 min for precipitation rate, and the most frequently occurring precipitation type in the last 10 min were used. A 3 h spin up period was removed from the REG data set and only the RUC 6 h forecast is compared in this work. It should be noted that runway crosswinds were not actually measured by instrumentation, nor outputted directly from the models. These were calculated for each runway by considering runway direction, wind speed and wind direction. Observational persistence data were generated using 10 min reduced instrument data. Climate data were generated using 30 years (1980–2009) of hourly observations at CYYZ and CYVR. One ‘climate’ value was produced *per* hour using 30 points by using the average value for temperature, RH and wind speed, and using the median value for wind direction, ceiling and visibility. The climate data were used to see if the model had any value over typical climatology for that station and the results should be used with extreme caution.

### 6.1. Continuous variables

Mean absolute (MAE) and mean (ME) errors are tabulated for the continuous variables: temperature, relative humidity, wind speed, wind direction, maximum wind and crosswind speeds. These errors are defined as:

$$\text{Mean Error (ME)} = \frac{1}{N} \sum_{i=1}^N (Fi - Oi) \quad (1)$$

$$\text{Mean Absolute Error (MAE)} = \frac{1}{N} \sum_{i=1}^N |Fi - Oi| \quad (2)$$

where  $F$  and  $O$  represent the forecasts and observations respectively.

The errors include all forecast lead times and times of day. The statistics generated here do not include REG or LAM model overlapping times; the most current model run is used and excludes the 3 h REG spin up time. For example, since LAM (east) was only run once *per* day (Table 4) the forecast data used could be up to 24 h old. For the REG, for the 0000 GMT run, model forecasts from 0300 GMT to 0900 GMT were used, and for the 1200 GMT run, forecasts from 1500 to 2100 GMT were used. There are three wind gust schemes used: (1) a modified version of the Brasseur (2001) scheme developed by (Jocelyn Mailhot, private communication) B01-JM; (2) a modified version of the Brasseur (2001) scheme developed by (Faisal Boudala, private communication) B01-B, and, (3) the RUC operational version.

These statistics provide a very average picture as model performance during significant events are washed out with long periods of uninteresting weather. Results for the mean absolute error (MAE) for CYYZ and CYVR are shown in Tables 5(a) and 6(a). Results for the mean error (ME) for CYYZ and CYVR are shown in Tables 5(b) and 6(b).

The wind direction mean absolute errors are large in Tables 5 and 6. This was possibly due to the inclusion of data with small wind speeds, so the analysis was re-done, limiting it to speeds greater than 5 kt. Tables 7 and 8 show the modified results for CYYZ and CYVR. After removing the low wind speeds, the wind direction MAE are reduced by 20–30% in the winter and 10–20% in the summer.

Table 5(a). The mean absolute error for continuous variables for CYYZ.

Variable	Winter CYYZ MAE				Summer CYYZ MAE			
	REG	LAM	RUC 6 h	CLI	REG	LAM	RUC 6 h	CLI
Temperature (° C)	1.7	2.3	1.9	3.9	1.5	1.7	1.1	3.0
Relative humidity (%)	10.5	9.0	12.3	11.0	8.5	7.9	7.9	10.3
Wind speed (m s <sup>-1</sup> )	1.6	1.2	1.4	1.8	1.4	1.4	1.2	1.6
Wind direction (°)	19.4	20.6	23.3	75.4	28.8	34.9	28.3	76.8
Max wind speed (m s <sup>-1</sup> )	2.3	2.4	1.7	N/A	2.3	2.6	1.5	N/A
Crosswind Rwy 1 (m s <sup>-1</sup> )	1.9	2.0	1.7	N/A	2.0	2.2	1.6	N/A
Crosswind Rwy 2 (m s <sup>-1</sup> )	1.9	2.0	1.7	N/A	2.0	2.2	1.6	N/A
Crosswind Rwy 3 (m s <sup>-1</sup> )	1.9	2.0	1.5	N/A	1.9	2.3	1.5	N/A

CLI refers to the error if a climate average were used as the predictor. See Sections 6.1 and 6.2 for a description of the model data used.



Table 5(b). The mean error for continuous variables for CYYZ.

Variable	Winter CYYZ ME				Summer CYYZ ME			
	REG	LAM	RUC 6 h	CLI	REG	LAM	RUC 6 h	CLI
Temperature (° C)	−1.2	−1.4	−1.5	−1.2	−0.5	−0.3	−0.2	−1.5
Relative humidity (%)	8.6	4.9	11.8	4.5	3.1	−1.1	5.9	1.1
Wind speed (m s <sup>−1</sup> )	−1.4	−0.2	−0.7	−0.4	−1.1	0.3	−0.4	−0.6
Wind direction (°)	5.6	5.1	3.1	−29.6	1.8	1.8	3.0	−13.3
Max wind speed (m s <sup>−1</sup> )	1.4	1.7	−0.2	N/A	0.5	1.3	−0.2	N/A
Crosswind Rwy 1 (m s <sup>−1</sup> )	0.8	1.0	0.1	N/A	0.2	0.6	−0.1	N/A
Crosswind Rwy 2 (m s <sup>−1</sup> )	0.8	1.0	0.1	N/A	0.2	0.6	−0.1	N/A
Crosswind Rwy 3 (m s <sup>−1</sup> )	0.9	1.2	−0.3	N/A	0.5	1.1	−0.1	N/A

CLI refers to the error if a climate average were used as the predictor. The maximum wind speed for REG and LAM were obtained using the B01-B method. See Sections 6.1 and 6.2 for a description of the model data used.

Table 6(a). The mean absolute error for continuous variables for CYVR.

Variable	Winter CYVR MAE					Summer CYVR MAE				
	REG	LAM	RUC 6 h	CLI	LAM1K	REG	LAM	RUC 6 h	CLI	LAM1K
Temperature (° C)	1.4	1.1	1.7	2.7	1.4	1.3	1.3	4.4	1.6	1.4
Relative humidity (%)	8.0	7.7	10.5	9.2	7.2	8.8	6.4	14.0	6.5	7.2
Wind speed (m s <sup>−1</sup> )	1.4	1.4	2.6	1.7	1.3	1.6	1.6	1.7	1.5	1.5
Wind direction (°)	40.8	42.4	48.3	55.5	42.6	39.1	44.2	48.6	59.5	46.3
Max wind speed (m s <sup>−1</sup> )	2.0	1.9	3.1	N/A	1.9	2.2	2.5	2.5	N/A	2.2
Crosswind Rwy 1 (m s <sup>−1</sup> )	1.8	1.4	1.9	N/A	1.4	1.4	1.5	1.5	N/A	1.4
Crosswind Rwy 2 (m s <sup>−1</sup> )	2.0	1.7	2.7	N/A	1.6	1.7	1.6	1.8	N/A	1.6

CLI refers to the error if a climate average were used as the predictor. The maximum wind speed for REG and LAM were obtained using the B01-B method. Note the Olympic LAM (1 km) was available for this period and the method of B01-JM was used. See Sections 6.1 and 6.2 for a description of the model data used.

Table 6(b). The mean error for continuous variables for CYVR.

Variable	Winter CYVR ME					Summer CYVR ME				
	REG	LAM	RUC 6 h	CLI	LAM1K	REG	LAM	RUC 6 h	CLI	LAM1K
Temperature (° C)	−1.2	−0.5	0.8	−1.0	−1.0	−0.5	−0.8	−4.4	0.5	−0.7
Relative humidity (%)	2.7	−1.9	−4.3	−1.4	1.1	−5.9	−0.3	13.8	−2.1	−2.8
Wind speed (m s <sup>−1</sup> )	−0.8	0.3	1.9	−0.2	−0.3	−1.1	−0.2	−0.9	−0.4	−0.3
Wind direction (°)	−8.1	1.9	17.7	8.3	−0.5	−4.2	2.7	11.5	6.9	6.6
Max wind speed (m s <sup>−1</sup> )	0.4	−0.6	2.1	N/A	−1.4	−1.3	−1.8	−2.1	N/A	−1.0
Crosswind Rwy 1 (m s <sup>−1</sup> )	0.7	0.0	0.9	N/A	−0.1	−0.7	−0.8	−0.6	N/A	−0.8
Crosswind Rwy 2 (m s <sup>−1</sup> )	0.9	0.0	1.3	N/A	−0.2	−0.3	−0.7	−1.1	N/A	−0.9

CLI refers to the error if a climate average were used as the predictor. See Sections 6.1 and 6.2 for a description of the model data used.

Table 7. Mean absolute error (left) and mean error (right) in wind direction at CYYZ calculated with all the data and then when wind speeds less than five knots are removed.

Model	Winter		Summer		Model	Winter		Summer	
	All WS	WS > 5 kt	All WS	WS > 5 kt		All WS	WS > 5 kt	All WS	WS > 5 kt
REG	19.4	14.9	28.8	23.3	REG	5.6	4.4	1.8	0.2
LAM	20.6	16.2	34.9	28.6	LAM	5.1	4.9	1.8	0.7
RUC 6 h	23.3	18.1	28.3	23.3	RUC 6 h	3.1	3.9	3.0	4.1

MAE and ME can also be calculated at different times of the day (TOD). This can expose diurnal trends and differences relating to model spin up. Only ~120 (90) values (1 *per* day for 4 (3) months) are used in the mean error statistic for winter (summer). Errors can be compared with observational

persistence curves at specific times of the day (0300, 0900, 1500, and 2100 UTC). As before, the statistics generated include all REG and LAM forecast lead times, do not include REG or LAM model overlapping times, and only the most current model run is used.

Table 8. Mean absolute error (left) mean error (right) in wind direction at CYVR calculated with all the data and then when wind speeds less than five knots are removed.

Model	Winter		Summer		Model	Winter		Summer	
	All WS	WS > 5 kt	All WS	WS > 5 kt		All WS	WS > 5 kt	All WS	WS > 5 kt
REG	40.8	28.9	39.1	32.3	REG	−8.1	−8.1	−4.2	−3.6
LAM	42.4	29.2	44.2	34.5	LAM	1.9	3.4	2.7	3.4
LAM 1K	42.6	29.7	46.3	36.4	LAM 1K	−0.5	3.8	6.6	8.3
RUC 6 h	48.3	38.3	48.6	44.5	RUC 6 h	17.7	20.8	11.5	12.6

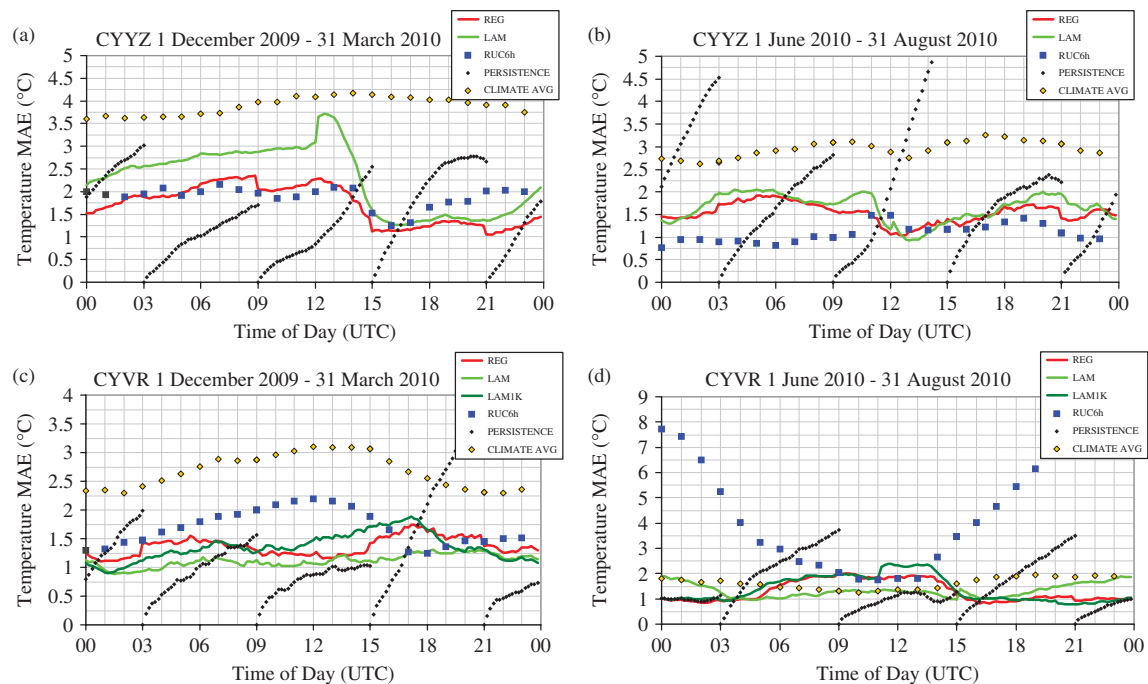


Figure 8. Shows the mean absolute errors in temperature as a function of time of day for CYYZ (a, b) and CYVR (c, d). (a) and (c) show the winter analysis and (b) and (d) show the summer analysis. A forecast using persistence is shown starting at 0300, 0900, 1500 and 1800 UTC.

Figures 8 and 9 show the time of day errors for temperature and wind speed gust for CYYZ and CYVR for both the winter and summer periods. It is clearly shown that the errors vary as a function of time of day. For some times, persistence can be the better forecast for up to 6 h.

Some highlights of the model continuous variable errors can be given. Wind direction errors at CYVR are considerably larger than at CYYZ. Summertime wind direction MAEs at CYYZ are noticeably larger than those in the winter time. Removing calm winds can reduce wind direction MAEs and reductions as large as 13° are seen. RUC summer temperature errors at CYVR are large and it is likely due to the choice of a model point which was a water point in this work. For CYVR, the nearest neighbouring RUC model grid point is only 1.5 km west of the observation site but the grid point approximately 11.5 km east of the observation site appears to verify better with the observations (Figure 10). This is because the nearest neighbour point was over the ocean. For the Canadian model points, only grid points over land were used in the forecasts. Unfortunately, for CYVR this was not done for the RUC model. The choice of model point appeared to not affect the wind speed and direction verifications for CYVR and this large difference was only seen in the summer. However, since airports are often located near water, selecting the best model grid point to represent the airport should be considered. Climate errors are

relatively large compared to the models for many variables and overall the climate data set should be used with caution. Without yet analysing error magnitudes (e.g. using block bootstrapping), it appears that the REG and LAM models perform similarly on average. Using these metrics and for the variables shown, LAM 1K at CYVR does not particularly outperform the 2.5 km LAM. However, more detailed studies have shown the value of the higher resolution model (see Mailhot *et al.*, 2012).

## 6.2. Categorical variables

A categorical analysis was performed for ceiling, visibility, precipitation rate, precipitation type, maximum wind and crosswinds for each runway. This was necessary because many of these variables are not continuous and it was necessary to do the analysis in bins or categories: these are shown in Table 9. They were chosen based on critical thresholds used in the Situation Chart. For visibility, three different schemes have been used: (1) the Gultepe and Milbrandt (2010) method modified with a visibility in snow scheme (GM10); (2) the Boudala and Isaac (2009) method (BI09), and, (3) the RUC operational version.

Many statistical tests were performed but only illustrations for the Heidke Skill Score (HSS) and accuracy score (ACC) are calculated. See the WWRP/WGNE Joint Working Group on Forecast Verification Research web pages for the definitions

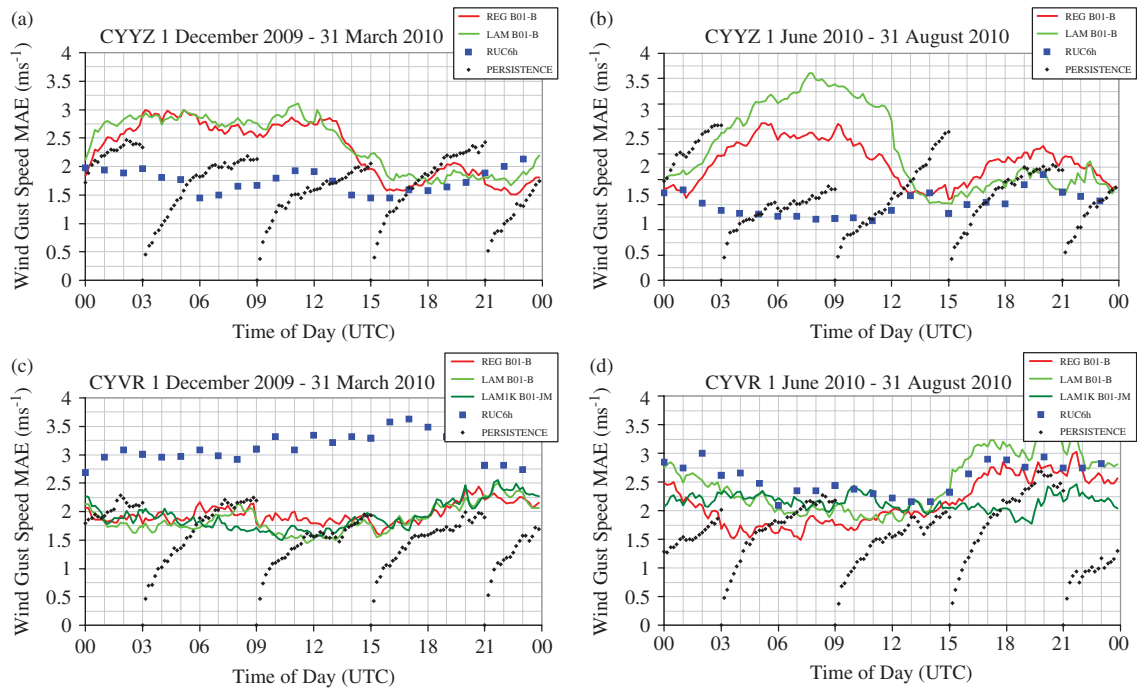


Figure 9. Shows the mean absolute errors in wind gust speed as a function of time of day for CYYZ (a, b) and CYVR (c, d). (a) and (c) show the winter analysis and (b) and (d) show the summer analysis. A forecast using persistence is shown starting at 0300, 0900, 1500 and 1800 UTC.

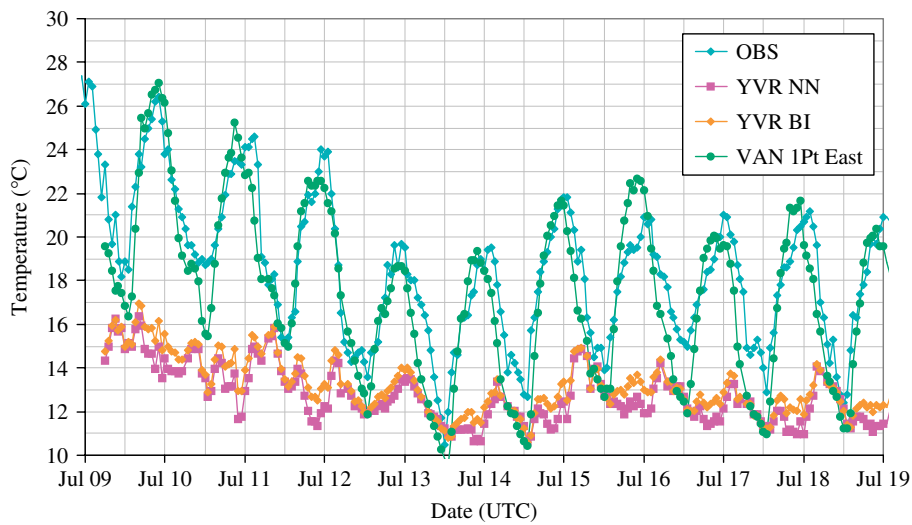


Figure 10. Shows the diurnal cycle for temperature at CYVR for a 10 day period in July 2010 (OBS) plotted against the U.S. RUC model nearest neighbour point 6 h prediction (YVR NN), the RUC point 13 km east of this point (VAN 1PtEast) and the bilinear interpolation between the two points (YVR BI).

of these scores. ([http://www.cawcr.gov.au/projects/verification/verif\\_web\\_page.html](http://www.cawcr.gov.au/projects/verification/verif_web_page.html)).

The multi-categorical (M-C) HSS score answers the question ‘What was the accuracy of the forecast in predicting the correct category, relative to that of random chance?’ with 1 indicating a perfect score and 0 no skill:

$$HSS = \frac{\frac{1}{N} \sum_{i=1}^k n(F_i, O_i) - \frac{1}{N^2} \sum_{i=1}^k N(F_i)N(O_i)}{1 - \frac{1}{N^2} \sum_{i=1}^k N(F_i)N(O_i)} \quad (3)$$

$N(F_i)$  represents the number of forecast points in the  $i$  category,  $N(O_i)$  represents the number of observations in the  $i$  category and  $N$  is the total number. The number of ‘hits’ in the  $i$  category is represented by  $n(F_i, O_i)$ .

The multi-categorical (M-C) ACC score answers the question ‘Overall, what fraction of the forecasts were in the correct category?’ with 1 indicating a perfect score and 0 no skill:

$$ACC = \frac{1}{N} \sum_{i=1}^k n(F_i, O_i) \quad (4)$$

where the symbols are the same as for Equation (3).

Table 9. Categories chosen for non-continuous variables as well as some critical continuous variables.

Variable	Category 1	Category 2	Category 3	Category 4	Category 5	Category 6	Category 7	Category 8
Winds	$< 5$ kt	$5 \leq w < 10$ kt	$10 \leq w < 15$ kt	$15 \leq w < 20$ kt	$20 \leq w < 25$ kt	$w \geq 25$ kt	–	–
Wind direction	$d \geq 339$ & $d < 24^\circ$ (N)	$24 \leq d < 69^\circ$ (NE)	$69 \leq d < 114^\circ$ (E)	$114 \leq d < 159^\circ$ (SE)	$159 \leq d < 204^\circ$ (S)	$204 \leq d < 249^\circ$ (SW)	$249 \leq d < 294^\circ$ (W)	$294 \leq d < 339^\circ$ (NW)
Visibility	$v < 1/4$ SM	$1/4 \leq v < 1/2$ SM	$1/2 \leq v < 3$ SM	$3 \leq v < 6$ SM	$v \geq 6$ SM	–	–	–
Ceiling	$c < 150$ ft	$150 \leq c < 400$ ft	$400 \leq c < 1000$ ft	$1000 \leq c < 2500$ ft	$2500 \leq c < 10\,000$ ft	$c \geq 10\,000$ ft	–	–
Precipitation rate	$r = 0$ mmh <sup>-1</sup> (none)	$0 < r \leq 0.2$ mmh <sup>-1</sup> (trace)	$0.2 < r \leq 2.5$ mmh <sup>-1</sup> (light)	$2.5 < r \leq 7.5$ mmh <sup>-1</sup> (moderate)	$r > 7.5$ mmh <sup>-1</sup> (heavy)	–	–	–
Precipitation type	No precipitation	Liquid	Freezing	Frozen	Mixed (w/liquid)	Unknown	–	–

The colours correspond to those used in the Situation Chart.

Table 10. Heidke Skill Score (HSS, top number) and accuracy score (ACC, bottom number) values for CYYZ for the winter and summer.

Variable	Winter CYYZ HSS and ACC			Summer CYYZ HSS and ACC		
	REG	LAM	RUC	REG	LAM	RUC
Ceiling	0.45	N/A	0.24	0.36	N/A	0.33
	0.62	N/A	0.47	0.63	N/A	0.67
Precipitation rate	0.30	0.29	0.40	0.23	0.18	0.18
	0.70	0.73	0.84	0.86	0.91	0.90
Visibility	N/A	N/A	0.22	N/A	N/A	0.16
	N/A	N/A	0.66	N/A	N/A	0.74
Visibility (BI09)	0.28	0.24	N/A	0.15	0.08	N/A
	0.75	0.75	N/A	0.78	0.80	N/A
Crosswind Rwy 1	0.27	0.27	0.30	0.21	0.17	0.31
	0.44	0.44	0.48	0.44	0.40	0.52
Crosswind Rwy 2	0.27	0.27	0.30	0.21	0.17	0.31
	0.44	0.44	0.48	0.44	0.40	0.52
Crosswind Rwy 3	0.29	0.26	0.32	0.22	0.18	0.30
	0.47	0.44	0.51	0.47	0.42	0.55
Precipitation type	0.46	0.47	N/A	0.36	0.29	N/A
	0.78	0.81	N/A	0.90	0.94	N/A
Maximum wind speed	0.18	0.19	0.30	0.07	0.11	0.29
	0.35	0.35	0.45	0.30	0.32	0.48
Wind direction	0.57	0.54	0.47	0.41	0.36	0.41
	0.64	0.62	0.56	0.49	0.45	0.50

The maximum wind speed for REG and LAM were obtained using the B01-B method.

Similar to the continuous variable verification described in Section 6.1, the overall and TOD statistics were generated using the non-overlapping GEM data set and include all GEM forecast lead times. The overall scores include all times of day. The scores are dominated by the most frequently occurring categories which are often the most uninteresting. Tables 10 and 11 show the HSS and ACC scores for the variables for both CYYZ and CYVR for the winter and summer periods.

Figures 11 and 12 show the Heidke Skill Scores (HSS) for ceiling and visibility, respectively, for CYYZ and CYVR. There is a large number of plots and graphs that can be shown from this work and the provided figures are just examples.

This type of analysis can be criticized because the model data and observations have to match exactly in time. The analysis

was redone by looking for the minimum (maximum) model value in  $\pm 60$  min of the observed time. For example, minimum visibility or cloud base height, and maximum precipitation rate were selected for the widened period. This is one method of ‘relaxing’ the comparison and it might improve statistics if it is thought that the model timing was a bit off (now given a 2 h window), if the model was more apt to overestimate ceiling or visibility, or if the model was more apt to underestimate precipitation rate. The results are shown in Table 12. The changes to HSS and ACC scores are small and not consistently for the better or worse.

Some conclusions regarding the categorical scores can be made. Similar to the continuous variables verification results, wind direction scores at CYYZ are higher than at CYVR. This includes persistence. REG ceiling scores seem to beat the

Table 11. Heidke Skill Score (HSS, top number) and accuracy score (ACC, bottom number) values for CYVR for the winter and summer.

Variable	Winter CYVR HSS and ACC				Summer CYVR HSS and ACC			
	REG	LAM	RUC	LAM1K	REG	LAM	RUC	LAM1K
Ceiling	0.41	0.31	0.32	0.28	0.51	0.18	0.23	0.23
	0.58	0.55	0.52	0.53	0.74	0.67	0.68	0.68
Precipitation rate	0.29	0.36	0.37	0.30	0.36	0.41	0.31	0.34
	0.65	0.74	0.81	0.66	0.92	0.94	0.95	0.91
Visibility (GM10 or RUC)	N/A	0.09	0.09	0.10	N/A	0.18	0.00	0.15
	N/A	0.69	0.63	0.68	N/A	0.93	0.53	0.92
Visibility (BI09)	0.08	0.08	N/A	0.12	0.24	0.23	N/A	0.16
	0.65	0.74	N/A	0.72	0.94	0.95	N/A	0.93
Crosswind Rwy 1	0.13	0.21	0.15	0.21	0.14	0.11	0.13	0.19
	0.56	0.69	0.58	0.70	0.65	0.64	0.62	0.62
Crosswind Rwy 2	0.17	0.21	0.02	0.22	0.16	0.16	0.08	0.21
	0.45	0.52	0.34	0.54	0.50	0.52	0.47	0.51
Precipitation type	0.44	0.52	N/A	0.52	0.51	0.58	N/A	0.60
	0.75	0.83	N/A	0.83	0.94	0.96	N/A	0.96
Maximum wind speed	0.20	0.20	0.09	0.15	0.08	0.04	0.01	0.13
	0.40	0.41	0.29	0.39	0.35	0.28	0.25	0.36
Wind direction	0.26	0.27	0.17	0.28	0.33	0.30	0.25	0.29
	0.41	0.45	0.41	0.46	0.44	0.40	0.36	0.40

The maximum wind speed for REG and LAM were obtained using the B01-B method and for LAM1K the B01-JM method was used.

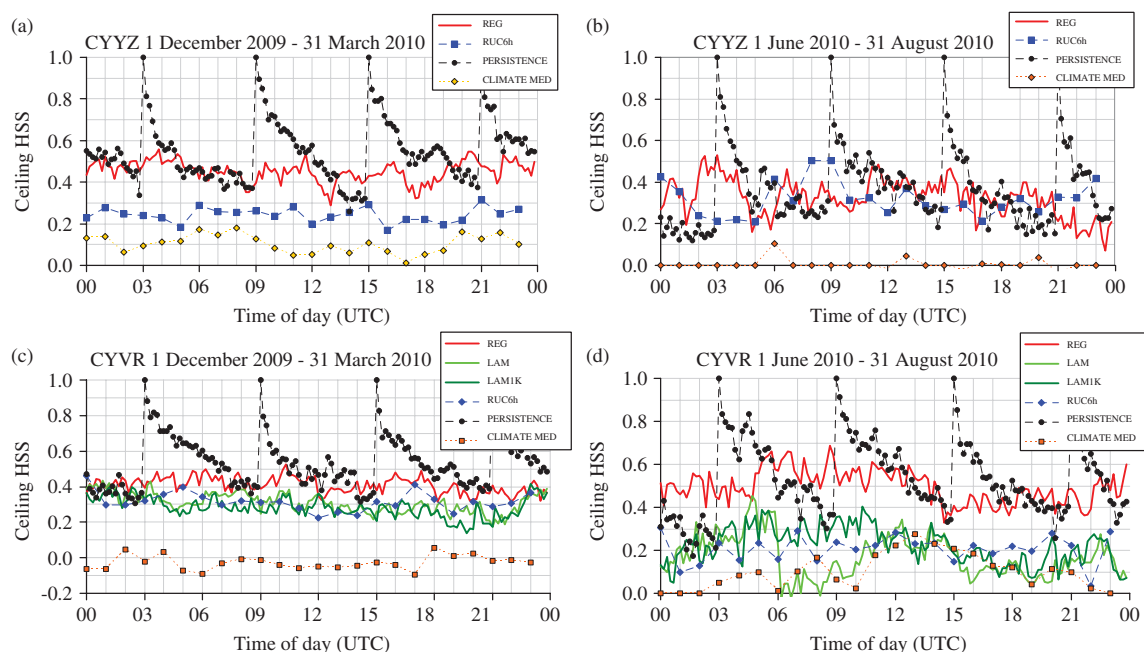


Figure 11. Shows the HSS for ceiling as a function of time of day for CYYZ (a, b) and CYVR (c, d). (a) and (c) show the winter analysis and (b) and (d) show the summer analysis. A forecast using persistence is shown starting at 0300, 0900, 1500 and 1800 UTC.

other models consistently. RUC 6 h wind gusts at CYYZ give higher scores than other models. CLIMATE scores for ceiling, visibility and winds are skill-less. LAM and LAM1K at CYVR perform similarly although one might expect LAM1K to have better scores. ‘Relaxing’ the analysis by a time window does not consistently improve or worsen scores. Multi-categorical scores stratified by time of day are interesting, but a lack of hits at various times leads to spiky and misleading scores (see CYVR visibility TOD plot, Figure 12). The multi-categorical scores are dominated by categories containing uninteresting weather such as no precipitation or unlimited ceilings.

## 7. Winter and summer verification of nowcast systems

This section will present some statistical verifications of the nowcast systems for lightning and icing forecasts, and the ABOM and INTW Nowcasts.

### 7.1. Lightning nowcasts

Lightning forecasts or nowcasts are prepared using the locations of the current lightning flashes and translating those positions forward 2 h in time (Figure 13). Note a ‘flash’ can have 1 to more than 20 strokes. A flash is translated in 1 h increments



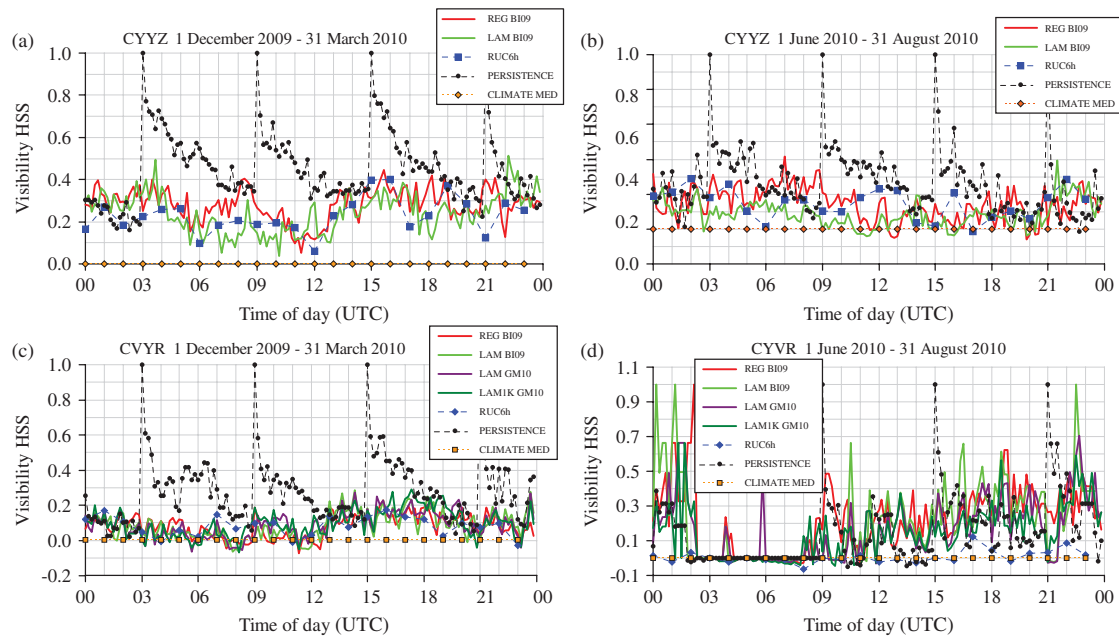


Figure 12. Shows the HSS for visibility as a function of time of day for CYYZ (a, b) and CYVR (c, d). (a) and (c) show the winter analysis and (b) and (d) show the summer analysis. A forecast using persistence is shown starting at 0300, 0900, 1500 and 1800 UTC.

Table 12. The Heidke skill score (HSS) and accuracy score (ACC) values for the relaxed set of criteria.

Model	Variable	CYYZ winter		CYYZ summer	
		Original M-C HSS/ACC	Relaxed M-C HSS/ACC	Original M-C HSS/ACC	Relaxed M-C HSS/ACC
REG	Ceiling	0.45/0.62	0.46/0.61	0.36/0.63	0.30/0.55
	Precipitation rate	0.30/0.70	0.26/0.62	0.23/0.86	0.19/0.78
	Visibility (BI09)	0.28/0.78	0.27/0.70	0.15/0.78	0.16/0.73
LAM	Precipitation rate	0.29/0.73	0.27/0.67	0.18/0.91	0.18/0.85
	Visibility (BI09)	0.24/0.75	0.25/0.71	0.08/0.80	0.11/0.77
RUC 6 h	Ceiling	0.24/0.47	0.25/0.45	0.33/0.67	0.33/0.63
	Precipitation rate	0.40/0.84	0.40/0.81	0.18/0.90	0.18/0.85
	Visibility	0.22/0.66	0.19/0.60	0.16/0.74	0.15/0.70

with vectors determined by the convective mode supported by the environment as the flash moves. An environment with bulk wind shear from the surface to 6 km exceeding 30 kt is deemed to support supercell growth. A supercell is translated with a left-moving vector or a right moving vector according to whether the directional wind shear in the cloud-bearing layer from the most unstable lifted parcel level (MU<sub>LPL</sub>) to 50% of the height between the MU<sub>LPL</sub> and the most unstable lifted parcel convective equilibrium level, is counter clockwise or clockwise (Bunkers *et al.*, 2000). A non-supercell may support new cell growth on the outflow boundary. Accordingly, a non-supercell is translated with the Corfidi vector (Corfidi, 1998) if the bulk wind shear from the surface to the most unstable lifted condensation level (MU<sub>LCL</sub>) is greater than 20 kt, otherwise it is translated with the mean wind vector from the MU<sub>LCL</sub> to 50% of the height between the MU<sub>LCL</sub> and the convective equilibrium level height. These forecasts are used to populate the Situation Chart by indicating how close lightning will come to the airport.

Lightning flash scatter plots for CYYZ are shown in Figure 14. For a 1000 km radius around the airport, the correlation co-efficient ( $r$ ) was 0.84. This reduced to  $r = 0.55$  for

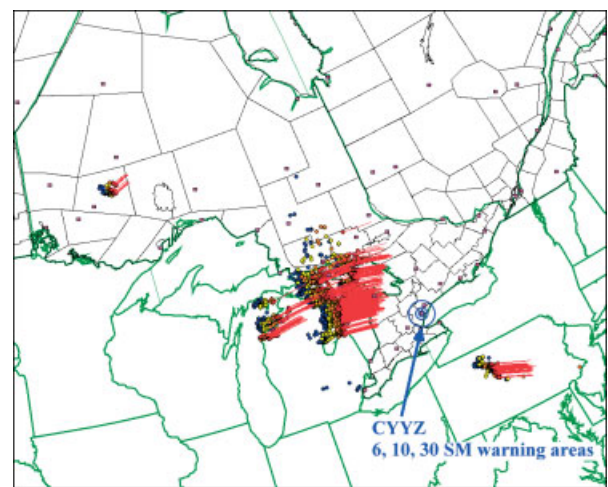


Figure 13. An example of the lightning nowcast map showing the 2 h forecast. The 6, 10 and 30 SM warning areas around Pearson (CYYZ) are shown.

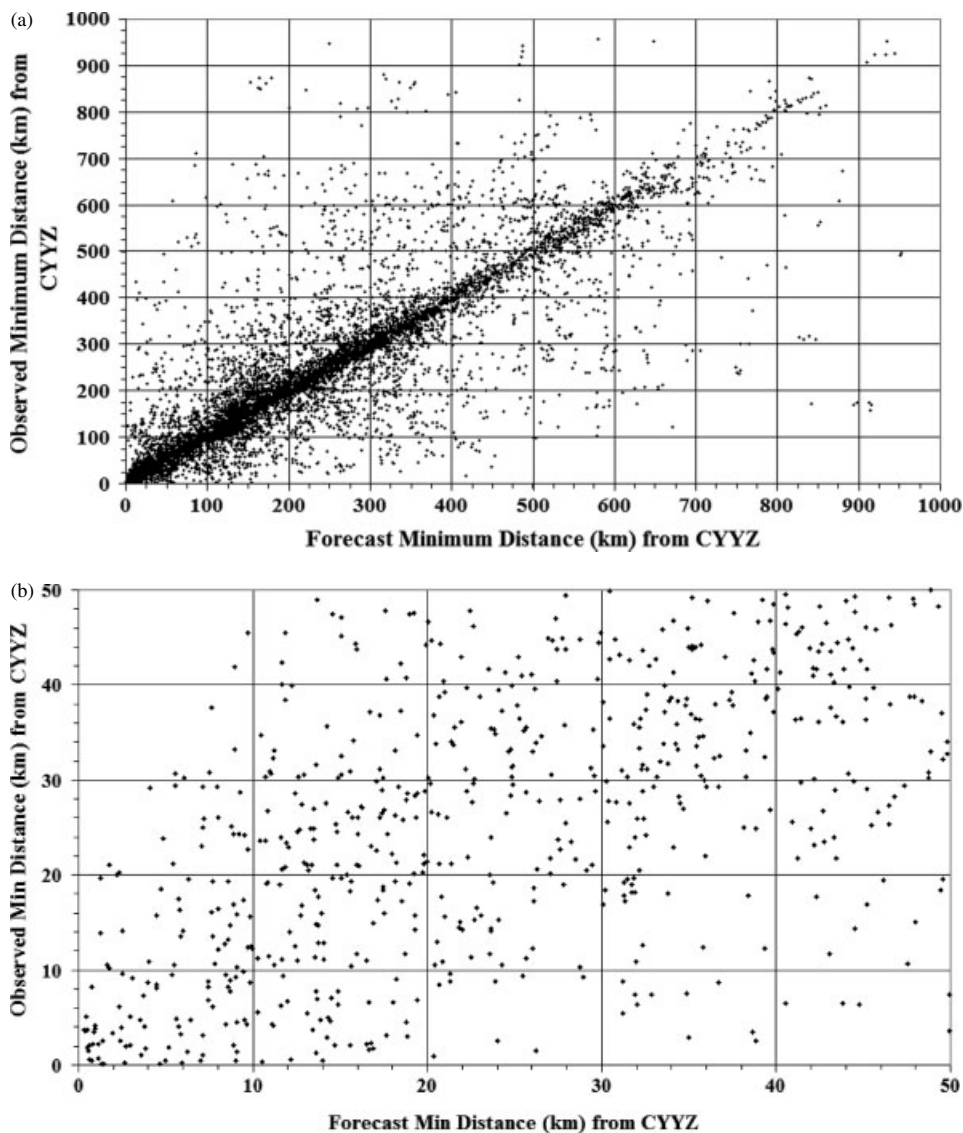


Figure 14. Verification of lightning forecasts for the summer of 2009 for CYYZ showing (a) the verification for flashes within 1000 km (the correlation co-efficient ( $r$ ) is 0.84) and (b) the zoomed portion within 50 km ( $r$  is 0.55).

a 50 km radius. It might be better to use motion vectors determined from weather radar images rather than model predictions, but that is a future development.

## 7.2. Icing forecasts

For each airport, icing is forecast above that airport using the GEM regional prediction of total water (liquid plus ice) content as a function of height and the freezing level. If there is a total water content greater than  $0.1 \text{ g m}^{-3}$  at temperatures colder than  $0^\circ\text{C}$ , the height of the lowest level and the total water content at that level is indicated and the Situation Chart indicates a potential icing aloft hazard. In terms of real time detection, a TP/WVP-3000 Microwave Radiometer (by Radiometrics) is located in the instrument compound at CYYZ and indicates the possible presence and amount of liquid water aloft. The co-located vertically pointing radar also has a detection algorithm which indicates the presence of drizzle aloft and if it occurs above the freezing level, supercooled drops are diagnosed.

## 7.3. Nowcasting precipitation amount and type

Nowcasting precipitation occurrence, rate and type during the winter are important for conveying useful information for those doing de-icing. The instrument site at CYYZ is directly across the runway from the de-icing pad (see Figure 2) so it is well suited to make the appropriate measurements. There is very little snow at CYVR in comparison to CYYZ (Figure 15), so the emphasis in this section will be on CYYZ.

To forecast precipitation type using the REG model, a modified version of the Bourgouin (2000) scheme was used. For the LAM runs in the west, the scheme as described by Milbrandt *et al.* (2008, 2010) was used. However, one problem is the actual measurement of precipitation type. It can vary quickly in time and the human observer may not pick up changes with a special report between the normal hourly observations. Figure 15 shows that different gauges can report different precipitation types, although the dominant types are clear, snow, rain, and drizzle. The Vaisala FD12P instrument reported more freezing rain and drizzle and ice pellets than the other instruments at CYYZ. This difference is significant and requires further study. It should be mentioned

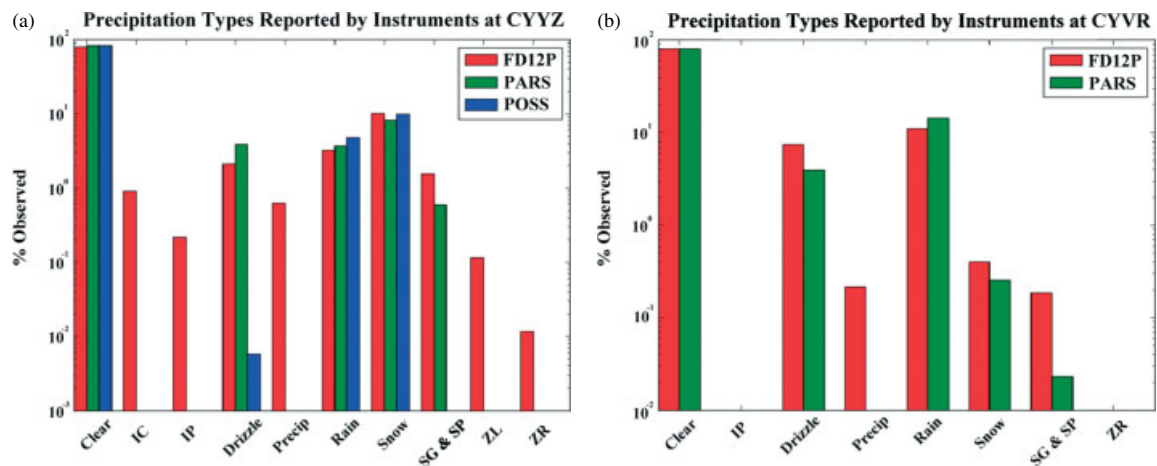


Figure 15. Percentage of time (log scale) precipitation types were observed at (a) CYYZ and (b) CYVR by three different instruments: the Vaisala FD12P, the OTT Parsivel and the POSS (Sheppard and Joe, 2008) averaged over the period 1 December 2009 to 31 March 2010. Types were determined at 10 min intervals.

that the instruments use the WMO definitions for precipitation type reporting. However, the models sometimes do not follow these definitions, with more sophisticated cloud microphysical schemes preferring to use graupel to define a range of precipitation particles such as small hail, ice pellets and snow grains. This also introduces problems in forecasting and verification.

Another significant problem is the measurement and forecast of rain or snow amount. Short term forecasts of precipitation amount can be made using scanning radars (see Figure 6(b)), but they require a 'Z-R' relationship which converts radar reflectivity to precipitation rate. This relationship is usually obtained through climatological averages and may have substantial errors for specific events. Sometimes this relationship can be tuned in real time with local gauges, but for snow it is very difficult to get an accurate snowfall amount over a short time scale. This makes such adjustments difficult and probably not precise.

Numerical models can also be used to forecast precipitation amount and Figure 16 shows an example of the cumulative amounts for the winter for REG and LAM compared with the Vaisala FD12P at CYYZ. The example shows good agreement, especially with REG, between the model and the instrument for the whole winter of 2009/2010, with significant differences during specific snow events. The climate normal for Pearson is about 102 cm of snow, so assuming that 1 mm of water equivalent is about 1 cm of snow, it shows that 2009/2010 received much less snow than normal.

#### 7.4. ABOM nowcasts

The Adaptive Blending of Observations and Models (ABOM) system was developed for CAN-Now (Bailey *et al.*, 2009). ABOM blends local surface based data with numerical weather prediction model outputs to generate nowcasts at a point location. The forecast at a specific time is based on the current

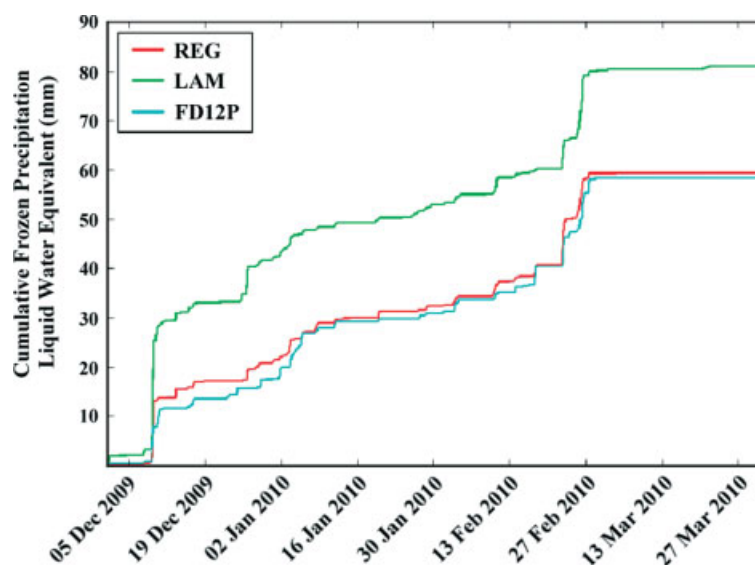


Figure 16. Shows the model REG and LAM cumulative snowfall amounts *versus* the Vaisala FD12P frozen precipitation (snow, snow grains, and ice pellets) for the winter of 2009/2010 at CYYZ. The precipitation amount is in mm water equivalent. The climate data, which are obtained from independent data sets, give 140 mm of rain and 52 cm of snow for same the 4 month period. The climate normals (1971–2000) are 119 mm rain and 102 cm of snow.

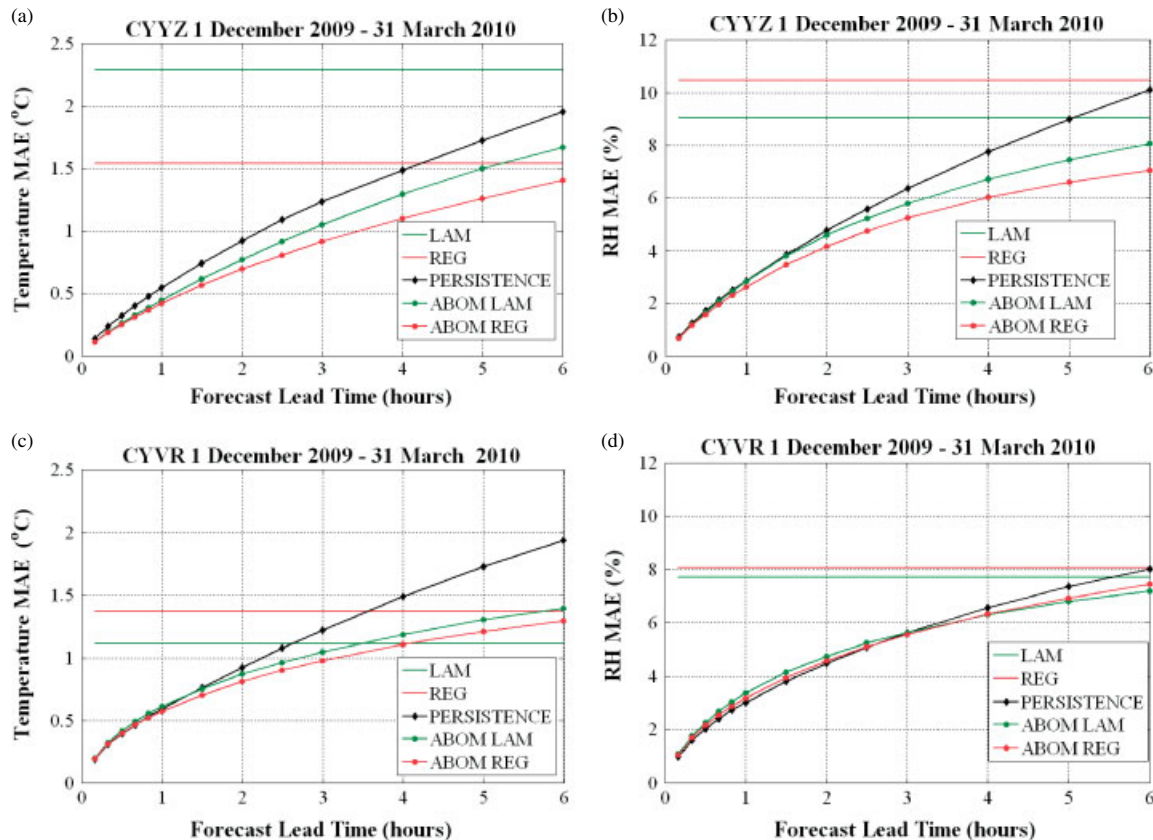


Figure 17. Shows the mean absolute error (MAE) in (a) temperature at CYYZ (b) RH at CYYZ (c) temperature at CYVR (d) RH at CYVR for the winter of 2009/2010 as a function of forecast lead time averaged over the whole season. Temperature and relative humidity ABOM REG and ABOM LAM are compared to the raw model output and persistence.

observation, the change predicted by the observation trend and the model trend. The basic equation is given below:

$$V_{k+p} = o_k + s_p(o_{k+p} - o_k) + r_p(m_{k+p} - m_k) \quad (5)$$

where  $V_{k+p}$  is the forecast at lead time  $p$ ,  $o_k$  is the current observation,  $s_p(o_{k+p} - o_k)$  is the change predicted by an observation trend and  $r_p(m_{k+p} - m_k)$  is the change predicted by the model. The co-efficients ( $s$  and  $r$ ) in the scheme are independent and trained using the recent history, typically 1 h, and are updated every 15 min. In the event that neither observation trend nor model change work well ( $s$  and  $r$  both near zero) the forecast defaults to observation persistence. Figure 17 shows the verification of ABOM for temperature and relative humidity for the winter of 2009/2010. It can be seen that ABOM using both the GEM and LAM NWP models outperforms persistence and the NWP model products by themselves.

### 7.5. INTW nowcasts

A Weighting, Evaluation, Bias Correction and Integrated System (WEBIS) has been developed for generating integrated weighted forecasts (INTW) from observations and NWP models for nowcasting (Huang, 2011; Huang *et al.*, 2012). The WEBIS adopts a new approach in blending the underlying model forecasts to improve overall forecast accuracy. As mentioned earlier, the system can examine several different NWP models, dynamically weigh those models based on past performance, and apply dynamic and variational bias corrections to produce a short term forecast to 6 h.

Tables 13 and 14 show MAE for continuous variables at CYYZ and CYVR for both the winter and summer periods based on the NWP models and the INTW 6 h forecasts. It is clear that the INTW system produces the best forecast at both CYYZ and CYVR.

Table 15 shows the models having the highest HSS score among all models for five categorical variables at CYYZ and CYVR in both winter and summer. Again, the INTW model is the best and most consistent performer among all models regardless of variable, season and location.

Figure 18 shows the mean absolute error in relative humidity and wind gust by nowcast lead time for the NWP models, persistence and INTW at CYYZ. Because of the averaging process, the numerical model errors are almost straight lines. Forecast errors in persistence and INTW grow with time for relative humidity and wind gust. For relative humidity, persistence and INTW beat the models out to 6 h. For wind gust, persistence beats the NWP model out to 3 h. However, the INTW system nowcast is the most accurate forecast out to 6 h. Generally, the INTW system outperforms the persistence forecast after 1 or 2 h and is the most accurate forecast out to 6 h for all variables.

The results of the study show that integrating surface observation data with the NWP forecasts produce better statistical scores than using either the raw NWP model forecasts or an objective analysis of observed data alone. Case studies have shown that INTW also produces better forecasts.

Another significant feature is that WEBIS can generate integrated forecasts very quickly and this allows dissemination of INTW in 'real' real-time. It takes only 2 s of generation time

Table 13. The mean absolute error for continuous variables for CYYZ and CYVR for the winter verification period for NWP models and INTW.

Variables	CYYZ MAE				CYVR MAE			
	REG	LAM	RUC	INTW	REG	LAM	RUC	INTW
Temperature ( $^{\circ}$ C)	1.7	2.3	1.9	1.0	1.4	1.1	1.7	0.8
Relative humidity (%)	10.5	9.0	12.3	5.4	8.0	7.7	10.5	5.0
Wind speed ( $\text{m s}^{-1}$ )	1.6	1.2	1.4	1.0	1.4	1.4	2.6	1.2
Max wind speed ( $\text{m s}^{-1}$ )	2.3	2.4	1.7	1.4	2.0	1.9	3.1	1.4
Crosswind Rwy 1 ( $\text{m s}^{-1}$ )	1.9	2.0	1.7	1.3	1.8	1.4	1.9	1.2
Crosswind Rwy 2 ( $\text{m s}^{-1}$ )	1.9	2.0	1.7	1.3	2.0	1.7	2.7	1.4
Crosswind Rwy 3 ( $\text{m s}^{-1}$ )	1.9	2.0	1.5	1.2	N/A	N/A	N/A	N/A

The maximum wind speed for REG and LAM were obtained using the B01-B method.

Table 14. The mean absolute error for continuous variables for CYYZ and CYVR for the summer verification period for NWP models and INTW.

Variables	CYYZ MAE				CYVR MAE			
	REG	LAM	RUC	INTW	REG	LAM	RUC	INTW
Temperature ( $^{\circ}$ C)	1.5	1.7	1.1	0.9	1.3	1.3	4.4	1.0
Relative humidity (%)	8.5	7.9	8.0	4.9	8.8	6.4	14.0	5.2
Wind speed ( $\text{m s}^{-1}$ )	1.4	1.4	1.3	1.0	1.6	1.6	1.7	1.1
Max wind speed ( $\text{m s}^{-1}$ )	2.3	2.6	1.5	1.5	2.2	2.5	2.5	1.4
Crosswind Rwy 1 ( $\text{m s}^{-1}$ )	2.0	2.2	1.6	1.5	1.4	1.5	1.5	1.1
Crosswind Rwy 2 ( $\text{m s}^{-1}$ )	2.0	2.2	1.6	1.5	1.7	1.6	1.8	1.2
Crosswind Rwy 3 ( $\text{m s}^{-1}$ )	1.9	2.0	1.5	1.4	N/A	N/A	N/A	N/A

The maximum wind speed for REG and LAM were obtained using the B01-B method.

Table 15. Model with highest HSS score among all models in CAN-Now for the winter and summer periods.

Variables	CYYZ		CYVR	
	Winter	Summer	Winter	Winter
Wind speed	INTW	INTW	INTW	INTW
Wind gust	INTW	INTW	INTW	INTW
Crosswind Rwy 1	INTW	INTW	INTW	INTW
Crosswind Rwy 2	INTW	INTW	INTW	INTW
Crosswind Rwy 3	INTW	INTW	INTW	INTW
Visibility	INTW	INTW	INTW	INTW
Ceiling	INTW	INTW	INTW	INTW
Precipitation rate	INTW	INTW	INTW	INTW

for 10 variables for one airport using a normal computer running a Linux operating system. For CAN-Now, INTW forecasts are updated frequently (every 10 min) and make use of newer data when it becomes available. Because of the verification scores obtained with INTW, it is currently used as the model for populating the Situation Chart.

## 8. Conclusions and possible future work

The CAN-Now system was evaluated with full field tests during the winter of 2009/2010 and the summer of 2010. The project attempted to verify statistically all the products it produces and this paper shows some of that work. Some basic conclusions can now be reached.

1. The web-based Situation Chart is a useful quick glance tool for alerting users to potential weather problems. Once

those problems have been identified, it is relatively easy to obtain more information and make appropriate decisions. As an example, if a significant wind shift is expected in the near future at the airport, perhaps due to a gust front or a frontal passage, then selection of an alternate runway by the Air Navigation Authority can be made more efficiently reducing operational problems. However, the Situation Chart is more complex than is necessary for some users in the airport environment, for example at the de-icing pad, so further improvements are necessary to get high-glance information to all users. Specific users generally require tailored displays focusing on their needs.

2. There is a need for measurements at high time resolution. Perhaps not adequately discussed in this paper, conditions at the airport can vary quickly on scales of several minutes. Relying on a human observer is not adequate although the human observations are also very useful given the uncertainties in the measurements.
3. There is a need for NWP model data at time resolutions better than 1 h for the same reason as mentioned above for the observations. Although perhaps not evident in this paper, higher spatial resolution models do, on average, provide more accurate forecasts (e.g. Mailhot *et al.*, 2012).
4. There is value in using more than one numerical weather forecast model in the products. Often one model captures a high impact event more accurately than another. The models are continuously being updated and there is a need to produce more probabilistic (ensemble) forecasts. Although the model and nowcast products have been statistically verified based on a season of data, it is necessary to do more comparisons and verifications for high impact events.



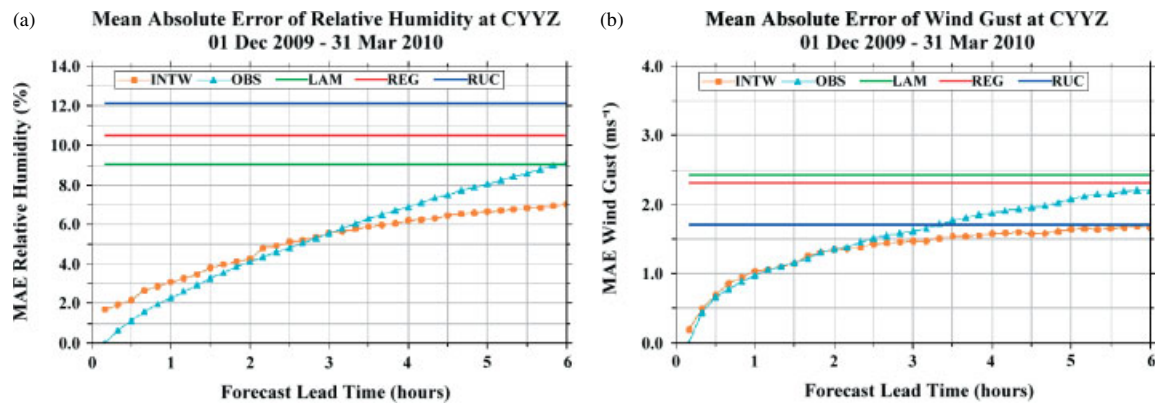


Figure 18. Shows the mean absolute error (MAE) in (a) relative humidity and (b) wind gust at CYYZ for the winter of 2009/2010 as a function of forecast lead time averaged over the whole season. Prediction using persistence is shown as OBS.

5. The nowcast systems developed have demonstrated skill. Currently, the INTW Nowcast system is used for the Situation Chart. However, further improvements in ABOM may show it to be very useful and it might be possible to blend the two techniques.
6. There is a great deal of future work necessary to measure precipitation amount and precipitation type more accurately. These are very critical parameters necessary in the application of de-icing fluids. Obviously, improvements in the ability to forecast these parameters are needed as well, but the current results are very promising (see Figure 16). The potential use of weather radar polarimetric data is being considered (Alliksaar *et al.*, 2010) for precipitation type forecasts using the local C-band operational radar which has dual polarization capability.
7. The forecast of vertical wind shear at the airport remains a significant problem, especially because the NWP models do not do a good job with this parameter (Zhou, 2010). Plans are underway to install and evaluate an acoustic boundary layer wind profiler at CYYZ. The possible use of AMDAR (Aircraft Meteorological Data Relay) data is also being considered.
8. There is a need to develop more spatial products around CYYZ and perhaps CYVR. Although forecasts are being shown for the airport bedposts, this is perhaps not sufficient. More upstream surface observations would also be useful.
9. The idea of using INTW and the various CAN-Now forecasts to produce a semi-automated First Guess TAF, for any airport, is now being actively studied. First results look very promising.
10. There is a need to bring in more forecaster involvement in using and modifying CAN-Now products. The CAN-Now website has a blog where forecaster and user comments can be made. In addition, there are text descriptions of the current weather (TAF Plus) prepared by the forecaster and available from the Situation Chart. However, more can be done.

## Acknowledgements

This work was funded by the National Search and Rescue Secretariat New Initiative Fund, Transport Canada, NAV CANADA, as well as Environment Canada. Special thanks must be given to Steve Bacic and Steve Brady for their skills in installing and maintaining equipment during the project. Our

colleagues at the Canadian Meteorological Centre and the Meteorological Research Branch in Montreal assisted us in getting and interpreting much of the numerical model data. Many of our colleagues at the Canadian Meteorological Aviation Centre offices in Edmonton and Montreal must also be mentioned including Stephen Kerr, Gilles Simard, Tim Guezen, and Bruno Larochelle. The authors also wish to thank Jean-Louis Brenguier and another anonymous reviewer for their useful comments on the manuscript.

## References

- Alliksaar M. 2010. Developing a hydrometeor-type point forecaster using polarimetric radar data, MSc thesis, Department of Earth and Space Science Engineering, York University, Toronto, Canada.
- Bailey ME, Isaac GA, Driedger N, Reid J. 2009. Comparison of nowcasting methods in the context of high-impact weather events for the Canadian Airport Nowcasting Project. *International Symposium on Nowcasting and Very Short Range Forecasting*, 30 August – 4 September 2009, Whistler, British Columbia.
- Bellon A, Austin GL. 1986. The accuracy of short-term radar rainfall forecasts. *J. Hydrol.* **70**: 35–49.
- Benjamin SG, Devenyi D, Smirnova T, Weygandt S, Brown JM, Peckham S, Brundage K, Smith TL, Grell G, Schlatter T. 2006. From the 13-km RUC to the rapid refresh. *12th Conference on Aviation, Range, and Aerospace Meteorology (ARAM)*, Atlanta, GA. CD-ROM, 9.1. American Meteorological Society: Boston, MA.
- Benjamin SG, Devenyi D, Weygandt SS, Brundage KJ, Brown JM, Grell GA, Kim D, Schwartz BE, Smirnova TG, Smith TL, Manikin GS. 2004. An hourly assimilation/forecast cycle: the RUC. *Mon. Weather. Rev.* **132**: 495–518.
- Boudala FS, Isaac GA. 2009. Parameterization of visibility in snow: application in numerical weather prediction models. *J. Geophys. Res.* **114**: D19202, DOI: 10.1029/2008JD011130.
- Boudala FS, Isaac GA, Crawford R, Reid J. 2012. Parameterization of runway visual range as a function of visibility: application in numerical weather prediction models. *J. Atmos. Oceanic Technol.* **29**: 177–191, DOI: 10.1175/JTECH-D-11-00021.1.
- Bourgouin P. 2000. A method to determine precipitation types. *J. Weather Forecast.* **15**: 583–592.
- Brasseur O. 2001. Development and application of a physical approach to estimating wind gusts. *Mon. Weather Rev.* **129**: 5–25.
- Bunkers MJ, Klimowski BA, Zeitler JW, Thompson RL, Weisman ML. 2000. Predicting supercell motion using a new hodograph technique. *Weather Forecast.* **15**: 61–79.
- Burrows WR, Kochtubajda B. 2010. A decade of cloud-to-ground lightning in Canada: 1999–2008. Part 1: flash density and occurrence. *Atmos. Ocean* **48**: 177–194.
- Corfidi SF. 1998. Some thoughts on the role mesoscale features played in the 27 May 1997 central Texas tornado outbreak. *Preprints, 19th Conference on Severe Local Storms, Minneapolis, MN*. American Meteorological Society: Boston, MA; 177–180.
- Côté J, Desmarais J-G, Gravel S, Méthot A, Patoiné A, Roch M, Staniforth A. 1998b. The operational CMC-MRB global environmental

- multiscale (GEM) model. Part II: results. *Mon. Weather Rev.* **126**: 1397–1395.
- Côté J, Gravel S, Méthot A, Patoine A, Roch M, Staniforth A. 1998a. The operational CMC-MRB global environmental multiscale (GEM) model. Part I: design considerations and formulation. *Mon. Weather Rev.* **126**: 1373–1396.
- Golding BW. 1998. Nimrod: a system for generating automated very short range forecasts. *Meteorol. Appl.* **5**: 1–16.
- Gultepe I, Milbrandt JA. 2010. Probabilistic parameterizations of visibility using observations of rain precipitation rate, relative humidity, and visibility. *J. Appl. Meteorol. Climatol.* **49**: 36–46.
- Gultepe I, Müller MD, Boybeyi Z. 2006. A new warm fog parameterization scheme for numerical weather prediction models. *J. Appl. Meteorol.* **45**: 1469–1480.
- Hansen B. 2007. A fuzzy logic-based analog forecasting system for ceiling and visibility. *Weather Forecast.* **22**: 1319–1330.
- Huang LX. 2011. Development of weighting, evaluation, bias correction and integrating system (WEBIS) for nowcasting, PhD dissertation, Department of Earth and Space Science and Engineering, York University, Toronto, Canada.
- Huang LX, Isaac GA, Sheng G. 2012. Integrating NWP forecasts and observation data to improve nowcasting accuracy. *Weather Forecast.* DOI:10.1175/WAF-D-11-00125.1 (in press).
- Isaac GA, Bailey M, Boudala F, Cober SG, Crawford R, Donaldson N, Gultepe I, Hansen B, Heckman I, Huang L, Ling A, Reid J, Fournier M. 2011. Decision making regarding aircraft de-icing and in-flight icing using the Canadian Airport Nowcasting System (CAN-Now). *SAE 2011 International Conference on Aircraft and Engine Icing and Ground Deicing*, 13–17 June 2011, Chicago, IL, Paper Number: 2011-38-0029; DOI: 10.4271/2011-38-0029.
- Isaac GA, Bailey M, Cober SG, Donaldson N, Driedger N, Glazer A, Gultepe I, Hudak D, Korolev A, Reid J, Rodriguez P, Strapp JW, Fabry F. 2006. Airport vicinity icing and snow advisor. *AIAA 44th Aerospace Sciences Meeting and Exhibit*, 9–12 January 2006, Reno, NV, AIAA-2006-1219.
- Lilly J, Côté C, Fabry F. 2004. Detection of aircraft icing environments with a Vertically Pointing Radar (VPR). *AIRS-II Workshop*, Mont Tremblant.
- Mailhot J, Bélair S, Lefaire L, Bilodeau B, Desgagné M, Girard C, Glazer A, Leduc A-M, Méthot A, Patoine A, Plante A, Rahill A, Robinson T, Talbot D, Tremblay A, Vaillancourt P, Zadra A, Qaddouri A. 2006. The 15 km version of the Canadian regional forecast system. *Atmos. Ocean* **44**: 133–149.
- Mailhot J, Milbrandt JA, Giguère A, McTaggart-Cowan R, Erfani A, Denis B, Glazer A, Vallée M. 2012. An experimental high-resolution forecast system during the Vancouver 2010 Winter Olympic and Paralympic Games. *Pure Appl. Geophys.* (in press).
- Milbrandt J, Yau MK, Mailhot J, Bélair S. 2008. Simulation of an orographic precipitation event during IMPROVE-2. Part I: evaluation of the control run using a triple-moment bulk microphysics scheme. *Mon. Weather Rev.* **136**: 3873–3893.
- Milbrandt J, Yau MK, Mailhot J, Bélair S, McTaggart-Cowan R. 2010. Simulation of an orographic precipitation event during IMPROVE-2. Part II: sensitivity to the number of moments in the bulk microphysics scheme. *Mon. Weather Rev.* **138**: 625–642.
- Rasmussen RM, Dixon M, Hage F, Cole J, Wade C, Tuttle J, McGettigan S, Carty T, Stevenson L, Fellner W, Knight S, Karplus E, Rehak N. 2001. Weather support to deicing decision making (WSDDM): a winter weather nowcasting system. *Bull. Am. Meteorol. Soc.* **82**: 579–595.
- Sheppard BE, Joe PI. 2008. Performance of the precipitation occurrence sensor system as a precipitation gauge. *J. Atmos. Oceanic Technol.* **25**: 196–212.
- Turnbull D, McCarthy J, Evans J, Zrnic D. 1989. The FAA Terminal Doppler Weather Radar (TDWR) program. *Preprints, Third International Conference on Aviation Weather Systems, Anaheim, CA*. American Meteorological Society: Boston, MA; 414–418.
- Ware R, Carpenter R, Guldner J, Liljegren J, Nehrkorn T, Solheim F, Vandenberghe F. 2003. A multichannel radiometric profiler of temperature, humidity, and cloud liquid. *Radio Sci.* **38**: 8079, DOI: 10.1029/2002RS002856.
- Zawadzki I, Fabry F, Szymer W. 2001. Observations of supercooled water and secondary ice generation by a vertically pointing X-band Doppler radar. *Atmos. Res.* **59–60**: 343–359.
- Zhou Y. 2010. Low level wind shear at two Canadian international airports, MSc thesis, Department of Earth and Space Science Engineering, York University, Toronto, Canada.